Datalogisk Institut
KØBENHAVNS UNIVERSITET

Steiner Trees for Fixed Orientation Metrics

Marcus Brazil and Martin Zachariasen

Technical Report no. 06/11
ISSN: 0107-8283

Dept. of Computer Science
University of Copenhagen • Universitetsparken 1
DK-2100 Copenhagen • Denmark

Steiner Trees for Fixed Orientation Metrics *

M. Brazil † M. Zachariasen‡

November 10, 2006

Abstract

We consider the problem of constructing Steiner minimum trees for a metric defined by a polygonal unit circle (corresponding to $\sigma \geq 2$ weighted legal orientations in the plane). A linear-time algorithm to enumerate all angle configurations for degree three Steiner points is given. We provide a simple proof that the angle configuration for a Steiner point extends to all Steiner points in a full Steiner minimum tree, such that at most six orientations suffice for edges in a full Steiner minimum tree. We show that the concept of canonical forms originally introduced for the uniform orientation metric generalises to the fixed orientation metric. Finally, we give a $O(\sigma n)$ time algorithm to compute a Steiner minimum tree for a given full Steiner topology with n terminal leaves.

Keywords: Steiner tree problem, normed plane, fixed orientation metric, canonical form, fixed topology.

1 Introduction

Given a fixed set of *legal* orientations in the plane, we consider the problem of constructing minimum-length interconnection networks with the restriction that

*Partially supported by a grant from the Australia Research Council and by a grant from the Danish Natural Science Research Council (51-00-0336).

†ARC Special Research Centre for Ultra-Broadband Information Networks, Department of Electrical and Electronic Engineering, The University of Melbourne, Victoria 3010, Australia

‡Department of Computer Science, University of Copenhagen, DK-2100 Copenhagen Ø, Denmark

line segments use legal orientations only. Furthermore, we assign *weights* to the legal orientations, such that the cost of a line segment is its length times its weight, and the total cost of the network is the sum of weighted line segment costs. This problem is equivalent to the *Steiner tree problem* under a metric that has a *polygonally* bounded unit circle.

The Steiner tree problem for fixed orientation metrics has important applications in VLSI design, where millions of nets should be routed on a (small) number of chip layers. Each layer is typically assigned a fixed orientation in order to make joint routing of multiple nets feasible. Traditionally only horizontal and vertical routing orientations have been used in chip production, but recent advances in production and routing algorithms have made it feasible to perform routing in more than two perpendicular orientations. The best known examples of such recent routing paradigms are the Y-architecture [8, 9] (where three uniformly distributed orientations are used) and the X-architecture [18, 20] (where four uniformly distributed orientations are used). Furthermore, there is a growing need for assigning weights to individual layers, such that some orientations can preferred or deferred [22].

In addition to applications in VLSI design, fixed orientation metrics can be used to *approximate* arbitrary metrics in the plane. As shown is this paper, increasing the number of legal orientations only increases the running times of computing Steiner minimum trees (SMTs) linearly. Therefore it is feasible to make tight approximations of arbitrary unit circles by polygonal unit circles.

Algorithms for solving several fixed orientation distance problems were proposed by Widmayer et al. [19]. For the Steiner tree problem, the rectilinear case — where two perpendicular orientations are given — has been studied most intensively due to its applications in traditional VLSI design [11, 12, 13, 24]. Important algorithms and fundamental properties for SMTs in uniform orientation metrics were given in [1, 2, 3, 16].

The Steiner tree problem in fixed orientation metrics is NP-hard, but when the topology of the tree is known, the problem can be solved in polynomial time by using linear programming [21, 25]. Moreover, for the uniform orientation problem with $\lambda \geq 2$ orientations (and assuming that the topology is full and has n terminal points as leaves) a $O(\lambda n)$ algorithm was proposed by Brazil, Thomas, Weng and Zachariasen [5]. The concept of forbidden subpaths from [3, 4] played a crucial role in achieving this fast algorithm.

In this paper we study the geometric structure of SMTs in order to show that they can be constructed in linear time when the topology of the tree is known. This is a significant generalisation of similar results for uniform orientation metrics [5].

The results in this paper also nicely complement similar results, such as those of Du et al. [10], for Steiner trees in any normed space defined by a strictly convex and differentiable unit circle.

We have endeavoured, in this paper, to find simple, direct proofs of these results. Particularly worthy of mention is Theorem 5.5, which shows that each full and fulsome component of an SMT only requires a small number of different orientations. Not only is this a key to establishing the canonical forms in the later parts of the paper, but it also provides a much simpler alternative proof to the less general and highly technical results on directions and forbidden subpaths in SMTs for uniform orientation metrics in [3, 4, 5]. Our paper essentially subsumes the main results of these papers, and many other structural results that have appeared in the literature on uniform orientation (including rectilinear) SMTs.

We begin by generalising the concept of direction sets from [5] to fixed orientation metrics and present a $\Theta(\sigma)$ time algorithm to enumerate all direction sets for an arbitrary fixed orientation metric with $\sigma \geq 2$ legal orientations. Then we show that direction sets extend throughout full SMTs — meaning that the edges in a full SMT use at most six legal orientations. In addition, we show that these full SMTs can be assumed to have certain canonical forms; one of these canonical forms has the property that the edges of a full SMT use at most four legal orientations. Furthermore, on the basis of the so-called depth-first order canonical form we give an $O(\sigma n)$ time algorithm to determine a SMT for a given full Steiner topology with n terminal leaves.

The paper is organised as follows. In Section 2 we define the Steiner tree problem in normed planes formally, present some known results and fix our notation. In Section 3 we present a useful geometric characterisation of meeting angles for Steiner points, and in Section 4 we introduce the concept of direction sets and show that we can identify all direction sets in $\Theta(\sigma)$ time. We show that a full SMT uses at most six legal orientations (coming from a single direction set) in Section 5. In Section 6 we give some fundamental results on length-preserving perturbations of Steiner points, and we introduce the concept of canonical forms for full SMTs. Based on these canonical forms, in Section 7 we devise a linear-time algorithm to compute a SMT for a given full Steiner topology. We conclude the paper in Section 8.

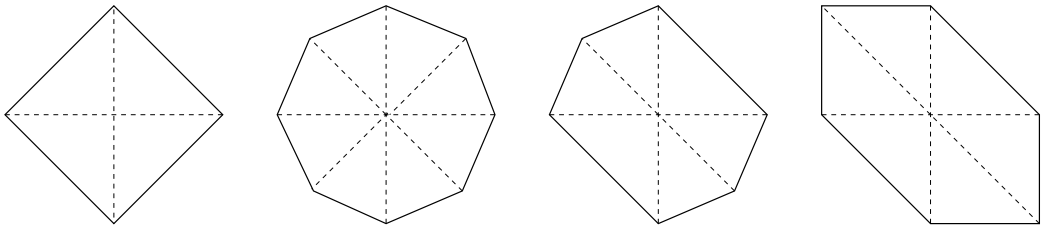

a) b) c) d)

Figure 1: Examples of polygonal unit circles. a) Rectilinear (2 perpendicular orientations). b) Uniform orientations ($\lambda = 4$). c) Non-uniform orientations ($\sigma = 3$). d) General weighted non-uniform orientations.

2 Preliminaries

We begin by setting some basic definitions and notation, and establishing generalisations of some important properties of SMTs for uniform orientation metrics. For a more detailed development of these properties, see [2, 5].

2.1 Normed Planes

Given a compact, convex, centrally symmetric domain $\mathcal{D}$ in the Euclidean plane E^2, one can define a norm $\|\cdot\|_{\mathcal{D}} : E^2 \to \mathbf{R}^+$ by setting $\|\mathbf{x}\|_{\mathcal{D}} = r$ where $\mathbf{x} = r\mathbf{u}$ and $\mathbf{u} \in \partial\mathcal{D}$, the boundary of $\mathcal{D}$. Denote the (closed) line segment joining distinct points $\mathbf{x}$ and $\mathbf{y}$ by $\mathbf{xy}$. We can then define a metric $|\cdot|_{\mathcal{D}}$ on E^2 by setting $|\mathbf{xy}|_{\mathcal{D}} = \|\mathbf{x}-\mathbf{y}\|_{\mathcal{D}}$. The resulting metric space $M = (E^2, |\cdot|_{\mathcal{D}})$ is called a *normed* (or *Minkowski*) plane with unit disc $\mathcal{D}$. By definition, $\partial\mathcal{D} = \{\mathbf{x} : \|\mathbf{x}\|_D = 1\}$, and is often referred to as the unit circle.

In this paper we will limit our attention to normed planes in which the unit circle $\partial\mathcal{D}$ is a centrally symmetric polygon. The best known example of this is the rectilinear plane [11] with norm $\|(a, b)\|_{\mathcal{D}} = |a| + |b|$. Here $\partial\mathcal{D}$ is a square whose two diagonals lie on the x-axis and y-axis respectively (Figure 1a). An important generalisation of the rectilinear plane is the λ-geometry plane [2], for each integer $\lambda(\geq 2)$, in which $\partial\mathcal{D}$ is a regular 2λ-gon (Figure 1b). Further generalisation is denoted fixed orientation geometry [19] (Figure 1c).

In the λ-geometry plane, or in any normed plane in which $\partial\mathcal{D}$ is a centrally symmetric 2σ polygon inscribed in a (Euclidean) unit circle, we can avoid the difficulties of computing directly with the associated metric as follows. We assume

that line segments are restricted to lying in σ distinct *legal orientations* corresponding to the σ diagonals of $\partial\mathcal{D}$. Then, for any pair of distinct points $\mathbf{x}$ and $\mathbf{y}$, the length of the shortest path between them composed of legal line segments is equal to $|\mathbf{xy}|_{\mathcal{D}}$. In other words, line segments in the normed plane can be represented by minimum paths composed of legal line segments in the Euclidean plane. See [19] for more details on the properties of such a representation. This will be our point of view throughout this paper.

As noted in [17], this idea can be extended to normed planes in which $\partial\mathcal{D}$ is any centrally symmetric 2σ polygon — not necessarily inscribed in a Euclidean unit circle (Figure 1d). Again line segments in the normed plane can be represented by paths composed of legal line segments, but now the total length of such a path is determined by weighting each legal line segment according to its orientation. The weighting on each line segment corresponds to the inverse of the distance of the corresponding vertex of $\partial\mathcal{D}$ from the centre of $\mathcal{D}$. One can again show, using similar arguments to those in [19], that the minimum length of such a path corresponds to the normed plane distance metric between its endpoints.

It is natural to ask whether this approach can be extended to any given set of σ orientations with given weights for each orientation. A potential problem is that the corresponding 2σ polygon may not be convex, meaning that we do not have a normed plane. However, we can circumvent this difficulty by considering the convex hull of the corresponding polygonal region. For any vertex of the 2σ polygon that does not lie on this convex hull, the corresponding orientation will never appear in a minimum path because a line segment in that orientation can always be replaced by line segments in other legal orientations at a smaller total cost. Hence, in this sense our approach is completely general for all finite sets of orientations and all possible weightings.

2.2 Steiner Trees in Normed Planes with Polygonally Bounded Unit Circle

Throughout this paper, we assume that a normed plane whose unit circle $\partial\mathcal{D}$ is a centrally symmetric polygon is given. Let $\sigma \geq 2$ denote the number of distinct legal orientations in the normed plane.

Given a set of points N (so-called *terminals*) in the plane, a *Steiner minimum tree (SMT)* is a shortest possible interconnection of N under the metric given by $\partial\mathcal{D}$. A SMT may contain vertices of degree three or more that are not among the given terminals; these vertices are denoted *Steiner points*.

The graph structure of a tree T (i.e., the pattern of adjacencies of the vertices for a given labelling of the terminals) is referred to as its *topology* $\mathcal{T}$. If, for the given norm, the total edge length of T, $|T|_{\mathcal{D}}$, is minimum for a given topology $\mathcal{T}$ (possibly in a degenerate way), then we say that T is a *SMT for* $\mathcal{T}$. For a fixed topology it follows that $|T|_{\mathcal{D}}$, treated as a function of the Steiner points of T, is a convex function (since T lies in a normed plane). Note, however, that this convexity is not strict; it may be possible to move Steiner points in a SMT without increasing the length of the tree.

A tree T or its topology $\mathcal{T}$ is said to be *full* if all its terminals have degree 1; if every Steiner point furthermore has degree three, then $\mathcal{T}$ is denoted a *full Steiner topology*. Given any SMT T, we can decompose T into full components, that is, into full SMTs that meet only at terminals. Furthermore, T or its topology $\mathcal{T}$ is said to be *fulsome* if T contains the maximum possible number of full components for any SMT on the terminal set of T. If we perturb the Steiner points in a fulsome SMT (without changing the length of the tree), then we cannot make a Steiner point coincide in position with one of the terminals. Clearly, for any set of terminals there always exists a SMT in which every full component is fulsome.

The edges of Steiner trees will be assumed to be represented by paths composed of line segments in legal orientations, as discussed in Section 2.1. It follows from [19] that each edge (u, v) of a Steiner tree uses at most two legal orientations; furthermore these two orientations are necessarily adjacent. When two legal orientations are required to represent an edge, then we call the edge a *bent edge*. Bent edges can be realised using exactly two legal line segments. There are two possible embeddings of such a path in the plane E^2, as shown in Figure 2a. A point (of degree 2) at which two legal line segments with different orientations meet is called a *corner point*. There are, of course, many other possible embeddings using multiple corner points, and the union of all these embeddings (or shortest paths) is a parallelogram $R(u, v)$. It is sometimes useful to consider an embedding with two corner points (as shown in Figure 2b) which has the property that the path has the same orientation at both endpoints.

3 Meeting Angles for Steiner Points

In this section we give a complete characterisation of the distribution of meeting angles of Steiner points in SMTs for a metric defined by unit circle $\partial\mathcal{D}$. Let $\mathbf{u}_l$, $l = 0, \ldots, 2\sigma - 1$ be the 2σ vectors that define the vertices of the unit circle $\partial\mathcal{D}$ (in counter-clockwise order around the circle). These are unit vectors in the metric

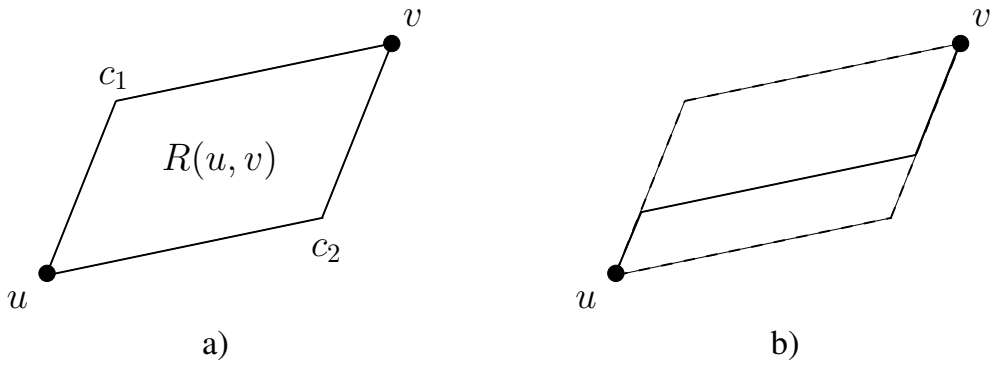

Figure 2: Embedding of a bent edge. a) The two embeddings uc_1v and uc_2v that only require two line segments (and a single corner point); the union of all shortest paths between u and v is denoted by $R(u, v)$. b) An embedding with identical orientations at endpoints.

given by $\partial\mathcal{D}$, that is, they have length 1 under metric $|\cdot|_{\mathcal{D}}$. By the central symmetry of $\partial\mathcal{D}$, we have that $\mathbf{u}_l = -\mathbf{u}_{(l+\sigma) \bmod 2\sigma}$. Each unit vector corresponds to a *legal direction*, that is, under this metric, any (oriented) legal line segment must use one of the 2σ unit vector directions. The *successor* of unit vector $\mathbf{u}_l$ is the vector $\mathbf{u}_{l+1}$ where $l + 1 := (l + 1) \bmod 2\sigma$, $l = 0, \ldots, 2\sigma - 1$.

In the remainder of this paper will make frequent use of the assumption that $\partial\mathcal{D}$ is placed somewhere in the plane such that its centre coincides with a given point s. For such a fixed centre we can unambiguously refer to the *vertices* of $\partial\mathcal{D}$, which are the endpoints of the unit vectors $\mathbf{u}_l$ for this fixed centre. The vertex that corresponds to the endpoint of unit vector $\mathbf{u}_l$ is denoted by u_l for $l = 0, \ldots, 2\sigma-1$.

3.1 Steiner Configurations

Following [17], we define a *Steiner configuration* in the normed plane as a star with centre s and leaves $x_1, \ldots, x_m$ (with $s, x_1, \ldots, x_m$ all distinct) that is part of some SMT with Steiner point s. By [17], Steiner points in a normed plane have degree at most 4, hence $m = 3$ or 4 in a Steiner configuration. Here we first consider the case where $m = 3$, and return to the (special) $m = 4$ case in Section 5.

Consider a star with Steiner point s and leaves x_1, x_2 and x_3. Assume w.l.o.g. that the counter-clockwise order of the leaves is x_1, x_2, x_3. We define the *meeting angles* of s to be the angles $\angle x_1sx_2$, $\angle x_2sx_3$ and $\angle x_3sx_1$, i.e., the angles that

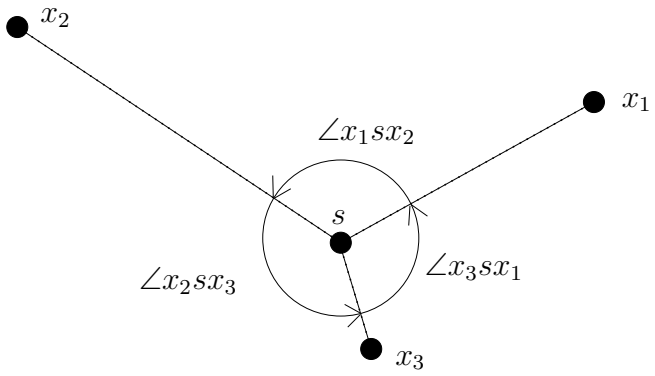

Figure 3: Meeting angles.

appear counter-clockwise around the Steiner point s (Figure 3).

Du et al. [10] proved the following result for strictly convex and differentiable unit circles (which includes the Euclidean metric): If one of the edges of the star, say sx_1, is given, then the orientations of the other edges sx_2 and sx_3 are *unique*. In other words, if Steiner point s and one of the leaves, say x_1, are given, then the meeting angles of s are unique. In this section we develop an analog version of this result for polygonal unit circles. We start with the following theorem from [14], which holds for any normed plane.

Definition 3.1 *An angle $\phi = \angle x_1 s x_2$ is* critical *if $\phi \leq \pi$ and there exists a point $x_3 \neq s$ such that Steiner point s with leaves x_1, x_2, x_3 forms a Steiner configuration, with $\phi = \angle x_1 s x_2$ as one of the meeting angles. (Compared to the definition of critical in [14] we have added the condition that the meeting angle is at most π.)*

Theorem 3.1 *[14] A star with centre s and leaves x_1, x_2, x_3 forms a Steiner configuration in a normed plane if and only if all meeting angles are critical.*

Chakerian and Ghandehari [7] gave a very useful characterisation of Steiner configurations for strictly convex and differentiable unit circles. If a unit circle is placed with its centre at s and l_1, l_2 and l_3 are the tangents of the unit circle where the rays $s \to x_1$, $s \to x_2$ and $s \to x_3$ intersect the unit circle, then l_1, l_2 and l_3 form a triangle whose *centroid* coincides with s. We say that the tangents l_1, l_2 and l_3 have the *centroid-property*. For more general unit circles, including polygonal unit circles, the tangents are not in general well-defined. However, by considering supporting lines instead of tangents, the following slightly weaker result can be proved for arbitrary normed planes (or unit circles):

Lemma 3.2 *[14] The following statements are equivalent in a normed plane with unit circle $\partial\mathcal{D}$:*

(i) $\angle x_1 s x_2$ is a critical angle

(ii) if the unit circle $\partial\mathcal{D}$ with centre s intersects the ray $s \to x_1$ at x_1' and the ray $s \to x_2$ at x_2', then there exist lines l_1, l_2 and l_3 supporting $\partial\mathcal{D}$, l_1 at x_1' and l_2 at x_2', such that s is the centroid of the triangle formed by l_1, l_2 and l_3 (or equivalently, l_1, l_2 and l_3 have the centroid-property).

3.2 Steiner Configurations for Fixed Orientation Metrics

Based on Lemma 3.2, we will give a characterisation of Steiner configurations for polygonal unit circles that is similar to the one shown by Chakerian and Ghandehari [7]. In order to do so, we need to characterise under which conditions a given supporting line l_1 of the unit circle can be a side in a triangle of supporting lines that has s as its centroid. Our characterisation will be based on the following condition on when set of supporting lines l_1, l_2 and l_3 has the centroid-property.

Lemma 3.3 *[10] Let l_0 be the line that is parallel to l_1 and contains s. Let Δ be the Euclidean distance between the parallel lines l_1 and l_0. Consider the line L that is parallel to l_1 at distance 3Δ from l_1 (and at distance 2Δ from l_0). Let w_2 be the intersection of l_2 with l_0 and let w_3 be the intersection of l_3 with l_0 (Figure 4a). Then supporting lines l_1, l_2 and l_3 satisfy the centroid property if and only if (i) lines l_2 and l_3 intersect somewhere on the line L, and (ii) $|sw_2| = |sw_3|$, where $|\cdot|$ denotes the Euclidean distance.*

In the following lemmas and theorems we will frequently refer to l_0 and L as defined by Lemma 3.3.

Lemma 3.4 *Let l_1, l_2 and l_3 be a set of supporting lines that fulfils the centroid-property, and let l_0 be the line that is parallel to l_1 and contains s. Then neither l_2 nor l_3 can support $\partial\mathcal{D}$ at a point that is strictly between l_1 and l_0.*

Proof. Assume that l_2 supports $\partial\mathcal{D}$ at a point x_2 that is strictly between l_1 and l_0 (Figure 4b), and let w_2 denote the intersection of l_2 with l_0. Consider the point y opposite to x_2 on $\partial\mathcal{D}$. By the central symmetry of $\partial\mathcal{D}$, there exists a line l_y supporting $\partial\mathcal{D}$ at y which is parallel to l_1 (Figure4b). Let w be the intersection of l_y with l_0. Clearly we have $|sw_2| = |sw|$.

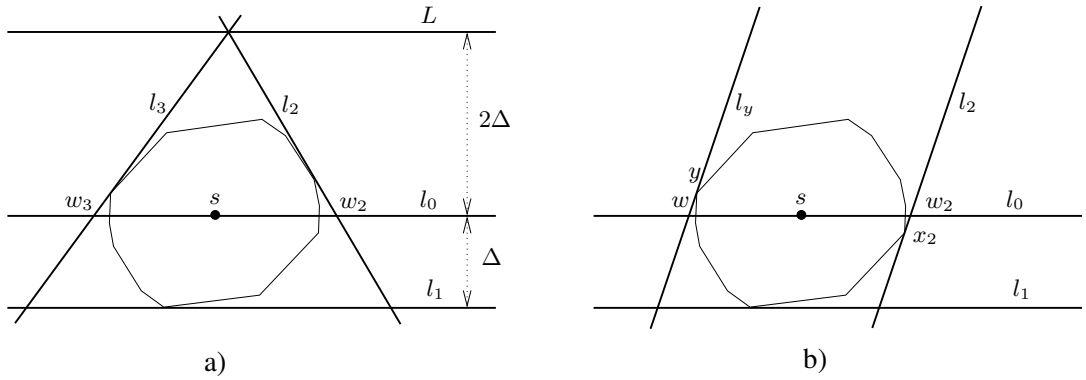

Figure 4: Illustration of proof of Lemma 3.4. a) Geometric characterisation of triangle with centroid s. b) Tangent l_2 cannot be part of a triangle with centroid s.

If supporting line l_3 exists, then it can be obtained by rotating l_y clockwise along the boundary of $\partial\mathcal{D}$. Since each of the rotation points are strictly above l_0, the distance $|sw|$ increases strictly as l_y is rotated. Thus we have that $|sw_3| > |sw_2|$, where w_3 is the intersection of l_3 with l_0. By Lemma 3.3, supporting lines l_1, l_2 and l_3 do therefore *not* have the centroid-property.

A similar result is obtained if l_3 supports $\partial\mathcal{D}$ at a point x_3 that is strictly between l_1 and l_0 — hence proving the lemma. ∎

Lemma 3.5 *Let l_1 be a line that supports a unit circle $\partial\mathcal{D}$ with centre s, and let l_0 be the line that is parallel to l_1 and contains s. If l_0 does* not *intersect a vertex of $\partial\mathcal{D}$ then there exists exactly* one pair *of supporting lines l_2 and l_3, such that l_1, l_2 and l_3 have the centroid-property.*

Proof. Consider the line l_2 supporting $\partial\mathcal{D}$ at one of the two intersections of l_0 with $\partial\mathcal{D}$ (Figure 5a). (Note that l_2 is in fact a tangent of $\partial\mathcal{D}$).

Let z be the intersection between l_2 and L. Define l_3 as the unique supporting line that contains z and supports $\partial\mathcal{D}$ on the "opposite" side to l_2, such that l_1, l_2 and l_3 form a triangle with s in its interior. Let w_2 (resp. w_3) be the intersection of l_2 (resp. l_3) with l_0 (Figure 5a).

Imagine rotating l_2 and l_3 jointly in a counter-clockwise manner around $\partial\mathcal{D}$, such that they continuously intersect L at a common point z (Figure 5b). This rotation strictly increases $|sw_2|$, while it strictly decreases $|sw_3|$, since all rotation points are strictly above l_0. The rotation is performed until l_3 is parallel to the original line l_2 (and thus supports the opposite point of $\partial\mathcal{D}$ that is also on l_0).

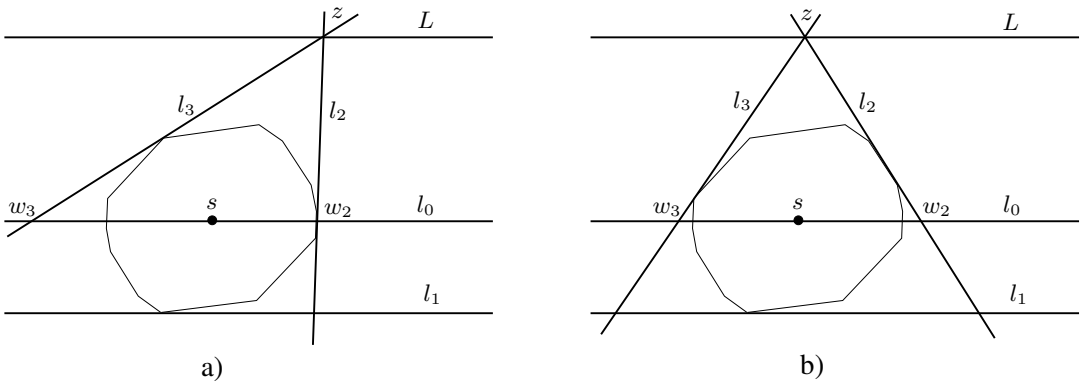

Figure 5: Illustration of proof of Lemma 3.5. a) Initial position of supporting lines. b) Intermediate position of supporting lines.

Before the rotation started we clearly had $|sw_2| < |sw_3|$, and when the rotation ends we have $|sw_2| > |sw_3|$. Hence, since both distances are strictly increasing/decreasing, there exists exactly one point z on L where the corresponding supporting lines l_2 and l_3 have $|sw_2| = |sw_3|$. By Lemma 3.3, for this and only this set of supporting lines the centroid-property holds. ∎

If, on the other hand, l_0 does intersect a vertex of $\partial\mathcal{D}$ then by the central symmetry of $\partial\mathcal{D}$ it intersects two vertices. We consider this case in the following lemma.

Lemma 3.6 *Let l_1 be a line that supports a unit circle $\partial\mathcal{D}$ with centre s, and let l_0 be the line that is parallel to l_1 and contains s. If l_0 intersects $\partial\mathcal{D}$ at two vertices u_j and u_k then either*

- *there exists exactly* one pair *of supporting lines l_2 and l_3, such that l_1, l_2 and l_3 have the centroid-property, or*
- *there exist an infinite set of supporting lines l_2 and l_3 such that l_1, l_2 and l_3 have the centroid-property, and in each case l_2 and l_3 support $\partial\mathcal{D}$ at u_j and u_k.*

Proof. Recall that u_j and u_k are the vertices of $\partial\mathcal{D}$ that are intersected by l_0. The predecessor of u_j (resp. u_k) on $\partial\mathcal{D}$ is u_{j-1} (resp. u_{k-1}) and the successor is u_{j+1} (resp. u_{k+1}).

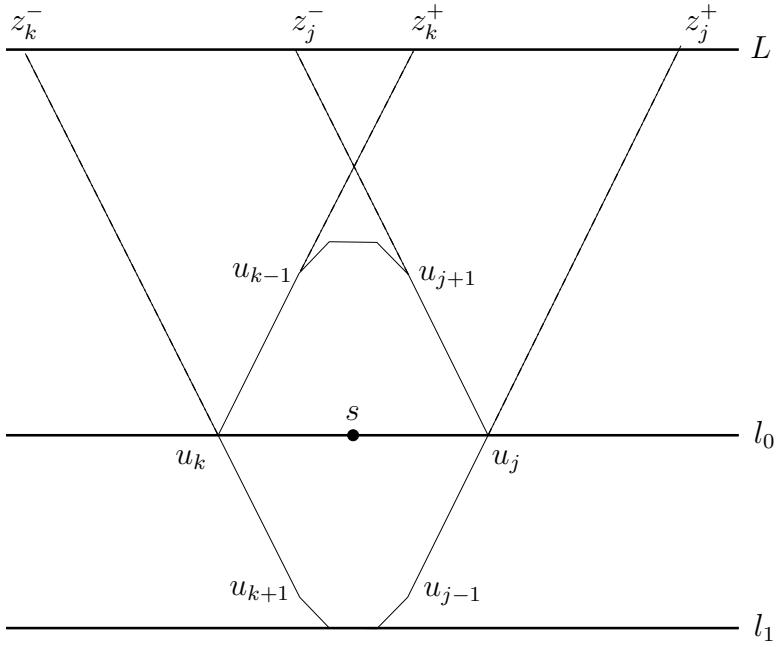

Figure 6: Illustration of proof of Lemma 3.6.

Let z_j^- be the intersection of the line through u_j and u_{j+1} with L, and let z_j^+ be the intersection of the line through u_{j-1} and u_j with L; define z_k^- and z_k^+ similarly (Figure 6).

Now we distinguish between three cases, depending on the order (from left to right) in which the points z_j^- and z_k^+ appear on L:

1. $z_j^- < z_k^+$: In this case any point z in the interval $[z_j^-, z_k^+]$ defines a pair of supporting lines l_2 and l_3 that contain z and support $\partial\mathcal{D}$ on opposite sides, such that l_1, l_2 and l_3 have the centroid-property. In this case we have an infinite number of supporting line pairs l_2 and l_3, and all these pairs support $\partial\mathcal{D}$ at u_j and u_k, respectively.

2. $z_j^- = z_k^+$: Here the point $z = z_j^- = z_k^+$ defines a pair of supporting lines l_2 and l_3 that contain z and support $\partial\mathcal{D}$ on opposite sides, such that l_1, l_2 and l_3 have the centroid-property. Note that l_2 supports $\partial\mathcal{D}$ both at u_j and u_{j+1} (is a tangent), and similarly l_3 supports $\partial\mathcal{D}$ both at u_k and u_{k-1}. In this case this is the only pair of supporting lines that jointly with l_1 have the centroid-property.

3. $z_j^- > z_k^+$: In this case there is clearly no pair of supporting lines that (jointly with l_1) have the centroid-property and support $\partial\mathcal{D}$ at either u_j or u_k. It follows that the method of proof of Lemma 3.5 applies to this case; hence, exactly one pair of supporting lines jointly with l_1 has the centroid-property. The common intersection point for this pair of supporting lines lies strictly between z_k^+ and z_j^- on L. ∎

We are now ready to prove the main result of this section — namely to make a precise link between the centroid-property and Steiner configurations for polygonal unit circles.

Theorem 3.7 *Consider a normed plane defined by a polygonal unit circle $\partial\mathcal{D}$, and a star $\mathcal{S}$ with centre s and leaves x_1, x_2 and x_3. In the unit circle with centre s, let x_1', x_2' and x_3' be the intersections with (the extensions of) the edges sx_1, sx_2 and sx_3, respectively. Assume that one of the intersections, say x_1', is* not *a vertex of the polygonal unit circle. Then $\mathcal{S}$ forms a Steiner configuration* if and only if *there exists a set of lines l_1, l_2 and l_3 supporting $\partial\mathcal{D}$ at x_1', x_2' and x_3', respectively, such that l_1, l_2 and l_3 have the centroid-property.*

Proof. Consider first the case where we have a set of supporting lines l_1, l_2 and l_3 that satisfy the centroid-property. By Lemma 3.2, each of the meeting angles in the star $\mathcal{S}$ are therefore critical angles, since we can use supporting lines l_1, l_2 and l_3 to prove this for all three meeting angles. Hence, by Theorem 3.1, the star $\mathcal{S}$ forms a Steiner configuration.

For the other direction, assume that $\mathcal{S}$ forms a Steiner configuration. All meeting angles of $\mathcal{S}$ are therefore critical by Theorem 3.1. For each meeting angle in $\mathcal{S}$, we know by Lemma 3.2 that there exist supporting lines having the centroid-property. However, these sets of supporting lines need not be identical: the supporting lines for, e.g., meeting angle $\angle x_1 s x_2$ support x_1' and x_2' on $\partial\mathcal{D}$, but need not support the third point x_3' on $\partial\mathcal{D}$. We will now prove that there indeed exists a set of supporting lines with the centroid-property supporting *all* three points x_1', x_2' and x_3' — thus finishing the proof of the theorem.

By the assumptions of the theorem we know that a supporting line of x_1' is necessarily a unique tangent; let l_1 denote this tangent. From Lemmas 3.5 and 3.6 we know that l_1 is either part of a *unique* set of supporting lines with the centroid-property *or* is part of an infinite set of such supporting lines. If l_1 is part of a *unique* set of supporting lines l_1, l_2 and l_3, then this set is the only one that proves that meeting angles $\angle x_1 s x_2$ and $\angle x_3 s x_1$ are critical. This set of supporting lines must therefore support $\partial\mathcal{D}$ in x_1', x_2' and x_3' simultaneously.

Now assume that there exists an infinite set of supporting lines l_1, l_2 and l_3 that have the centroid-property. By Lemma 3.6, we have the situation illustrated in Figure 6. Each possible supporting line l_2 supports some fixed vertex u_j of $\partial\mathcal{D}$, and each possible supporting line l_3 supports another fixed vertex u_k of $\partial\mathcal{D}$. As a consequence, x_2' must be somewhere on the line segment S_j of $\partial\mathcal{D}$ defined by vertices u_j and u_{j+1}; similarly, x_3' must be somewhere on the line segment S_k defined by vertices u_{k-1} and u_k. There are three cases to consider:

- $x_2' = u_j$: In this case we can pick l_3 such that it overlaps with S_k, and choose l_2 such that l_1, l_2, and l_3 have the centroid-property. Since l_3 overlaps with S_k, it supports any possible point x_3' on S_k.

- $x_3' = u_k$: This case is symmetric to the above — here we let l_2 overlap with S_j and choose l_3 accordingly.

- $x_2' \neq u_j$ and $x_3' \neq u_k$: This case *cannot* occur, since the angle $\angle x_2 s x_3$ is not critical. The reason is that the tangents l_2 and l_3 must overlap with S_j and S_k, respectively. However, there exists no third supporting line l_1 such that l_1, l_2 and l_3 have the centroid-property. The intersection point between l_2 and l_3 is strictly between the lines l_0 and L (in Figure 6), hence the third edge of the triangle must intersect the interior of the unit circle. ∎

The theorem requires that one of the intersections with the unit circle appears at a *tangent* point. However, this is no restriction as will be clear from the discussion in next section (in particular Lemma 4.1).

4 Direction Sets

For any Steiner configuration of degree $m = 3$ there is an associated set of legal directions, namely the legal directions used by all edges in the star (where directions are considered as oriented outward from the centre). A Steiner configuration $\mathcal{S}$ is said to be *maximal* if there exists no other Steiner configuration that uses a strict superset of the legal directions used by $\mathcal{S}$. We define a *direction set* to be the set of legal directions used by a maximal Steiner configuration. Note that in λ-geometry these direction sets are the same as the 'feasible direction sets' defined in [5].

For a direction set $\mathcal{U}$ we define the *complementary* direction set as the direction set that is obtained by reversing all directions in $\mathcal{U}$ (Figure 7). By the central symmetry of $\partial\mathcal{D}$, direction sets appear as *pairs* of complementary direction sets.

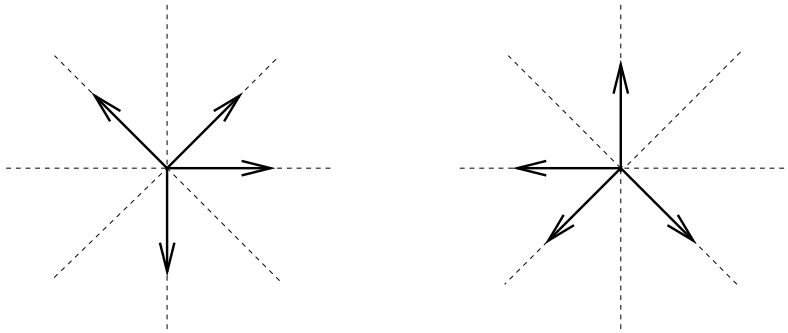

a) b)

Figure 7: Complementary direction sets in λ-geometry for $\lambda = 4$.

Lemma 4.1 *A direction set contains at least* 4 *and at most* 6 *distinct directions.*

Proof. The upper bound is obvious if $m = 3$, since each edge uses at most two legal directions. We establish the lower bound using a continuity argument.

Suppose, contrary to the claim of the lemma, there exists a direction set $\mathcal{U}$ with only 3 directions. Let T be a SMT with 3 terminals, t_1, t_2, t_3 and a Steiner point s, such that T has direction set $\mathcal{U}$. By convexity, the choice of s is unique, since if there were a second Steiner point s' that gave a SMT then every point in the line segment ss' would also be the Steiner point of an SMT. This would mean that a larger direction set strictly containing $\mathcal{U}$ could be found by moving the Steiner point from s a small distance towards s'.

For all points p in the plane define the function $f(p) := |t_1p|_{\mathcal{D}}+|t_2p|_{\mathcal{D}}+|t_3s|_{\mathcal{D}}$. Since T is a SMT it follows that, for every p, $f(p) \geq f(s) = |T|_{\mathcal{D}}$. For every $\varepsilon > 0$, let B_ε be the open Euclidean ball centre s and radius ε. By the continuity of f it follows that for each ε there exists $\delta = \delta(\varepsilon) > 0$ such that $f(p) > f(s) + \delta$ for all $p \notin B_\varepsilon$. Clearly we can also assume that $\delta < \varepsilon$.

Now choose $\varepsilon > 0$ sufficiently small such that perturbing one or both endpoints of each edge t_is by at most ε results in an edge in the normed plane that still uses a direction from $\mathcal{U}$ (for $i \in \{1, 2, 3\}$). Suppose we move terminal t_1 to t_1' not on the line through t_1s such that $0 < |t_1t_1'|_{\mathcal{D}} < \delta(\varepsilon)$ and such that T', the SMT for t_1', t_2, t_3, satisfies $|T'|_{\mathcal{D}} \leq |T|_{\mathcal{D}}$. Let s' be a Steiner point for T'. Then

$$\begin{aligned} f(s') &\leq |T'|_{\mathcal{D}} + |t_1t_1'|_{\mathcal{D}} \\ &< |T|_{\mathcal{D}} + \delta. \end{aligned}$$

Hence s' lies in B_ε. By our choice of ε it follows that $\mathcal{U}'$, the direction set of T', contains $\mathcal{U}$ as a subset (since the endpoints of the three edges of T have each been perturbed by at most ε). Since exactly one of the terminals of T has been perturbed it is easy to see that $\mathcal{U}$ is a strict subset of $\mathcal{U}'$, contradicting the statement that $\mathcal{U}$ is a direction set. ∎

A maximal Steiner configuration always has at least one edge that contributes two legal directions to the corresponding direction set (by Lemma 4.1). As in [5] we colour one such edge red and the other edges green and blue, respectively, in counter-clockwise order from the red edge. We extend these colour labels to the directions in the direction set. A direction set with coloured directions is denoted a *coloured* direction set. A coloured direction set always contains two red directions and these are adjacent legal directions. For a given colour, we therefore have either one or two legal directions in a coloured direction set. When we have two directions, these are labelled as the (exclusively) *primary* and the (exclusively) *secondary* direction, respectively, in counter-clockwise order around the unit circle. When we have a single direction for a given colour, this direction can be labelled either primary or secondary.

Assume we fix a pair of adjacent red directions, which correspond to two unit vectors $\mathbf{u}_i$ and $\mathbf{u}_{i+1}$ of $\partial\mathcal{D}$. How many coloured direction sets exist for this pair of red edges? Using Lemmas 3.5 and 3.6 we can prove that there exist either *one* or *two* direction sets for a fixed pair of red directions. For the case considered in Lemma 3.5 there is exactly *one* direction set which is given by the unit vectors whose endpoints are supported by the unique supporting lines l_1, l_2 and l_3 having the centroid-property (where l_1 supports $\partial\mathcal{D}$ at the endpoints of $\mathbf{u}_i$ and $\mathbf{u}_{i+1}$). For the first subcase considered in Lemma 3.6 (Figure 6) there are exactly two direction sets: One corresponding to a pair of green directions $\mathbf{u}_j$ and $\mathbf{u}_{j+1}$, and a single blue direction $\mathbf{u}_k$; the other corresponding to a single green direction $\mathbf{u}_j$ and a pair of blue directions $\mathbf{u}_{k-1}$ and $\mathbf{u}_k$. The other positions of l_2 and l_3 do not give direction sets as in each case the corresponding set of directions is not maximal. For the remaining subcases of Lemma 3.6 there is exactly one direction set. We summarise:

Theorem 4.2 *There are at least 2σ and at most 4σ coloured direction sets, where σ is the number of legal orientations defined by $\partial\mathcal{D}$. More precisely, there are k pairs of complementary coloured direction sets, where $\sigma \leq k \leq 2\sigma$.*

In the remainder of this section, we first develop an $O(\sigma^2)$ time algorithm to determine all (coloured) direction sets for a given polygonal unit circle $\partial\mathcal{D}$

defining σ legal orientations (and thus having 2σ unit vectors). Finally, at the end of this section we give an optimal $\Theta(\sigma)$ time algorithm for determining all coloured direction sets.

4.1 Quadratic-time Algorithm

In this section we give a $O(\sigma)$ time algorithm to determine all coloured direction sets for a *fixed* pair of red directions. By the arguments of Theorem 4.2, there is either one direction set or two direction sets for a fixed pair of red directions. By iterating over all 2σ choices of adjacent red directions, we can identify *all* coloured direction sets in $O(\sigma^2)$ time.

Let $\mathbf{u}_i$ and $\mathbf{u}_{i+1}$ be a pair of red directions (here and in the following we identify directions with the unit vectors of $\partial\mathcal{D}$). In order to determine the direction set(s) for this pair of red directions, we employ the construction used in the proof of Lemma 3.5.

Let l_1 be the tangent supporting $\partial\mathcal{D}$ at u_i and u_{i+1}, and define l_0 and L as in Section 3.1. In counter-clockwise order around $\partial\mathcal{D}$, starting at u_{i+1}, let u_j be the first vertex that is on or above l_0. Define $l_2(z)$ as the tangent supporting $\partial\mathcal{D}$ at u_{j-1} and u_j (Figure 8a), where z denotes the intersection of $l_2(z)$ with L. Let $l_3(z)$ be the other supporting line of $\partial\mathcal{D}$ that intersects z (Figure 8a). Line $l_3(z)$ either supports $\partial\mathcal{D}$ at a single vertex u_k, or at two adjacent vertices u_{k-1} and u_k. Clearly, given l_1, the supporting lines $l_2(z)$ and $l_3(z)$ can be determined in $O(\sigma)$ time.

Now we simulate a continuous movement of the point z to the left along L. Let $w_2(z)$ and $w_3(z)$ be the intersections of $l_2(z)$ and $l_3(z)$, respectively, with l_0 (Figure 8a). Note that initially we have $|sw_2(z)| < |sw_3(z)|$, where s is the centre of $\partial\mathcal{D}$. The movement of z is continued until we have a point z^* such that $|sw_2(z^*)| = |sw_3(z^*)|$, that is, until we fulfill the centroid-property; by Lemmas 3.5 and 3.6 such a point must exist. After initialisation the algorithm is as follows:

1. Define z_j as the intersection of the line supporting $\partial\mathcal{D}$ at u_j and u_{j+1} with L; similarly, define z_k as the intersection of the line supporting $\partial\mathcal{D}$ at u_k and u_{k+1} with L (Figure 8b). Note that both z_j and z_k are strictly to the left of z on L; let z' be the one of these two (possibly identical) points that is closest to z.

2. If $|sw_2(z')| < |sw_3(z')|$: If $z_j = z'$ then set $j = j + 1$. If $z_k = z'$ then set $k = k + 1$. Set $z = z'$ and goto 1.

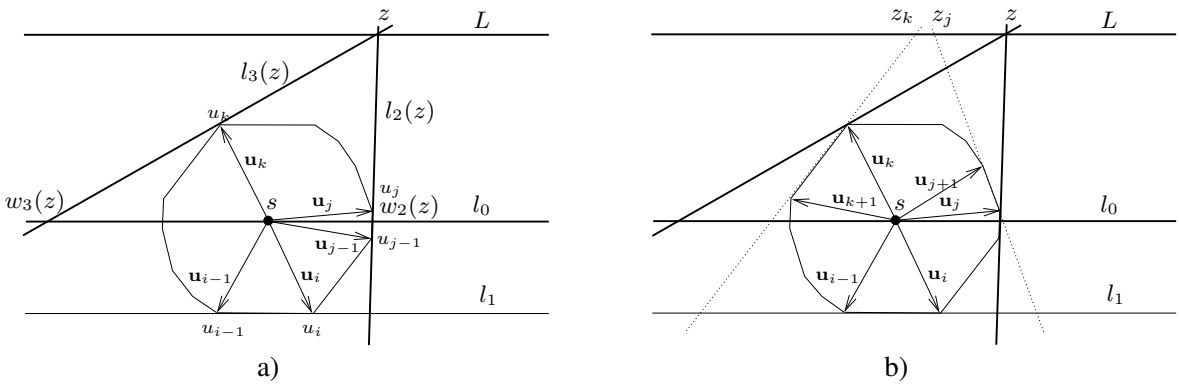

Figure 8: Algorithm to determine direction set for fixed pair of red directions. a) Initial position of z. b) Computation of z_j and z_k.

3. If $|sw_2(z')| > |sw_3(z')|$: The point z^* where $|sw_2(z^*)| = |sw_3(z^*)|$ must lie strictly between z and z' on L. Hence there is a *unique* direction set where $\mathbf{u}_{i-1}$ and $\mathbf{u}_i$ are the two red directions: $\mathbf{u}_j$ is the single green direction and $\mathbf{u}_k$ the single blue direction (4 directions in total).

4. If $|sw_2(z')| = |sw_3(z')|$:

   (a) $z_j = z'$ and $z_k \neq z'$: Here we have a *unique* direction set where $\mathbf{u}_{i-1}$ and $\mathbf{u}_i$ are the two red directions: $\mathbf{u}_j$ and $\mathbf{u}_{j+1}$ form a pair of green directions and $\mathbf{u}_k$ the single blue direction (5 directions in total).

   (b) $z_j \neq z'$ and $z_k = z'$: If either u_j or u_{k+1} are not on the line l_0 through s, then we have a *unique* direction set where $\mathbf{u}_{i-1}$ and $\mathbf{u}_i$ are the two red directions: $\mathbf{u}_k$ and $\mathbf{u}_{k+1}$ form a pair of blue directions and $\mathbf{u}_j$ a single green direction (5 directions in total). If both u_j and u_{k+1} are on the line l_0 through s, then we have *two* direction sets where $\mathbf{u}_{i-1}$ and $\mathbf{u}_i$ are the two red directions: The one just described, and one where $\mathbf{u}_j$ and $\mathbf{u}_{j+1}$ form a pair of green directions and $\mathbf{u}_{k+1}$ is a single blue direction (5 directions in total). Note that in this case we have $u_j = w_2(z')$ and $u_{k+1} = w_3(z')$.

   (c) $z_j = z_k = z'$: Here we have a *unique* direction set where $\mathbf{u}_{i-1}$ and $\mathbf{u}_i$ are the two red directions: $\mathbf{u}_j$ and $\mathbf{u}_{j+1}$ form a pair of green directions and $\mathbf{u}_k$ and $\mathbf{u}_{k+1}$ form a pair of blue directions (6 directions in total).

The above algorithm clearly takes $O(\sigma)$ time, since steps 1 and 2 take constant

time, and are iterated at most 2σ times: in each iteration j and/or k is increased, and there are at most σ possibilities for each iterator.

Theorem 4.3 *The direction sets (one or two) for a given pair of red directions can be determined in $O(\sigma)$ time. Thus all coloured direction sets can be determined in $O(\sigma^2)$ time.*

4.2 Linear-time Algorithm

The idea of the linear-time algorithm to determine all coloured direction sets is first to compute a set of supporting lines l_1, l_2 and l_3 for a fixed pair of red directions $\mathbf{u}_i$ and $\mathbf{u}_{i+1}$ using the $O(\sigma)$ time algorithm from the previous section. Intuitively, we then *rotate* all three supporting lines in counter-clockwise order around $\partial\mathcal{D}$ *while maintaining the centroid-property*, locating all positions of the supporting lines that correspond to direction sets. In order to prove that this can be done efficiently, we need some definitions and technical results.

Consider a line l_1 that supports $\partial\mathcal{D}$ at a single vertex u_i. We say that u_i is the rotation point of l_1. Consider a counter-clockwise rotation of l_1 around its rotation point. We continue this rotation until l_1 also supports the successor u_{i+1} of u_i. Then u_{i+1} becomes the new rotation point, and we continue the counter-clockwise rotation. This is called a rotation of l_1 around $\partial\mathcal{D}$.

Each step in the algorithm will strictly rotate around $\partial\mathcal{D}$ at least one of the supporting lines l_1, l_2 and l_3 that fulfill the centroid-property. However, not all supporting lines necessarily rotate in every step. The important fact that we will prove in Lemma 4.4 below is that none of the supporting lines need to rotate *clockwise* in order to maintain the centroid-property. Furthermore, in each step of the algorithm — which takes constant time — at least one of the supporting lines will change its rotation point to the successor on $\partial\mathcal{D}$ of the previous rotation point; such a supporting line will after the rotation step be a *tangent* supporting both the previous and new rotation point. Thus the running time of the algorithm is clearly $O(\sigma)$, since each supporting line has exactly 2σ possible rotation points.

Two types of constant-time rotation steps are used by the algorithm where the latter is only performed if the former cannot be performed.

Degenerate rotation Consider any of the current supporting lines l_1, l_2 and l_3. If this supporting line is part of more than one set of supporting lines fulfilling the centroid-property, then we have the situation considered in case 1 in the proof of Lemma 3.6 and illustrated in Figure 6. In this case we simply rotate the other two

supporting lines counter-clockwise as much as possible; in Figure 6 the situation after this rotation corresponds to the case where one of the lines supports $\partial\mathcal{D}$ at u_j and u_{j+1}, while the other line only supports $\partial\mathcal{D}$ at u_k.

Non-degenerate rotation Consider the current supporting lines and assume that their rotation points are u_i, u_j and u_k, respectively. Imagine that we rotate l_1 maximally counter-clockwise while maintaining the centroid-property and the invariant that l_1, l_2 and l_3 support $\partial\mathcal{D}$ at u_i, u_j and u_k, respectively. In Lemma 4.4 we prove that this *cannot* force l_2 and l_3 to rotate clockwise around their rotation points (i.e., in the "opposite" direction). A rotation of l_1 therefore must lead to one of the following events:

- l_1 becomes a tangent through u_i and u_{i+1}
- l_2 becomes a tangent through u_j and u_{j+1}
- l_3 becomes a tangent through u_k and u_{k+1}

Consider the event that l_1 becomes a tangent through u_i and u_{i+1}. We know that l_2 and l_3 must support $\partial\mathcal{D}$ at u_j and u_k, respectively. Thus we need to determine if there exists a set of supporting lines fulfilling the centroid-property, where l_1 is a tangent through u_i and u_{i+1}, l_2 supports $\partial\mathcal{D}$ at u_j and l_3 supports $\partial\mathcal{D}$ at u_k. This problem can be solved in constant time using a simple geometric construction as shown in Figure 9. The interval $I = I_j \cap I_k$ on L must be non-empty, and among the points $z \in I$ there should be one for which the supporting lines through z have identical distances on l_0 to s. This can be tested in constant time by constructing the supporting lines for the two endpoints of I. (Note that we need not compute the correct location of z, but only show that it exists.)

By using a similar constant-time construction we can test if if there exists a set of supporting lines fulfilling the centroid-property, where l_1 supports $\partial\mathcal{D}$ at u_i, l_2 is a tangent through u_j and u_{j+1}, and l_3 supports $\partial\mathcal{D}$ at u_k. Finally, we can also test in constant-time if there exists a set of supporting lines fulfilling the centroid-property, where l_1 supports $\partial\mathcal{D}$ at u_i, l_2 supports $\partial\mathcal{D}$ at u_j, and l_3 is a tangent through u_k and u_{k+1}. If more than one set of supporting lines exist, we choose one among the sets in lexicographical order, that is, choose the set where l_1 is a tangent first, then the one where l_2 is a tangent and finally the one where l_3 is a tangent.

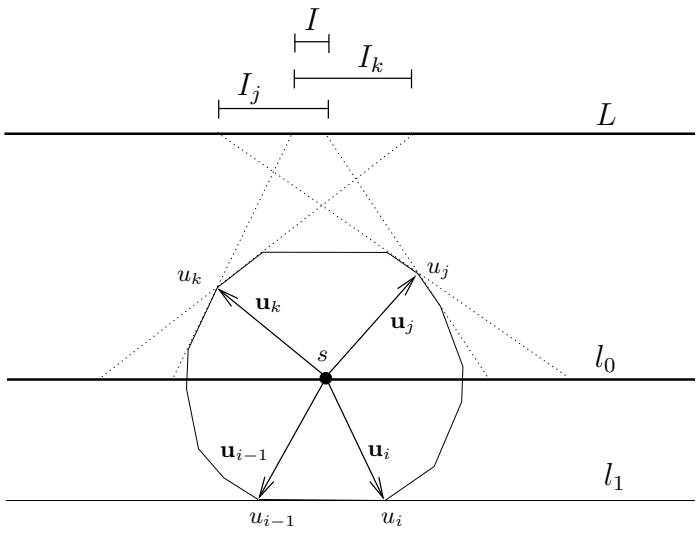

Figure 9: Constant-time construction to determine if there exists a set of supporting lines fulfilling the centroid-property, where l_1 is a tangent through u_i and u_{i+1}, l_2 supports $\partial\mathcal{D}$ at u_j and l_3 supports $\partial\mathcal{D}$ at u_k.

Lemma 4.4 *If we rotate l_1 counter-clockwise while maintaining the centroid-property and the invariant that l_1, l_2 and l_3 support $\partial\mathcal{D}$ at u_i, u_j and u_k, respectively, then neither l_2 nor l_3 can rotate in clockwise direction.*

Proof. Assume to the contrary that as we rotate l_1 counter-clockwise, l_2 rotates (strictly) clockwise. Let (l_1^A, l_2^A, l_3^A) be the set of supporting lines before we started this rotation. As we continue the rotation of l_1 (possibly via succeeding rotation points) around $\partial\mathcal{D}$, we reach a point where l_2 is "pushed back" to its original position. That is, we have another a set of supporting lines (l_1^B, l_2^B, l_3^B) that fulfils the centroid-property where $l_2^B = l_2^A$. But since l_1^B is rotated strictly more counter-clockwise than l_1^A, this a contradiction to the fact that we should have rotated l_1^A in a degenerate rotation step when we had the set of supporting lines (l_1^A, l_2^A, l_3^A).

A similar argument can be used to prove that l_3 cannot rotate clockwise as we rotate l_1 counter-clockwise. ∎

Theorem 4.5 *The set of coloured direction sets can be determined in $\Theta(\sigma)$ time.*

5 Directions in a full SMT

The aim of this section is to show that the edges in a full SMT use at most 6 legal orientations. This will prove to be a powerful result for developing canonical forms in later parts of the paper. Steiner points in any normed plane have degree $m = 3$ or $m = 4$ [17]. In this section we first show that if the full SMT is fulsome, then we may assume that all Steiner points have degree $m = 3$ (except in a very special case). Then we prove that there exists a single direction set that is used by every (degree three) Steiner point in a full and fulsome SMT.

5.1 Splitting of Degree Four Steiner Points

A degree four Steiner point s consists of two opposite pairs of edges. Let the neighbours of s be denoted by v_1, v_2, v_3 and v_4 in counter-clockwise order around s. One of the opposite pairs of edges, say, (s, v_1) and (s, v_3) must be *collinear* [17]; this is called the *first* pair of opposite edges. The other pair of edges, (s, v_2) and (s, v_4), is called the *second* pair of opposite edges. Our classification into pairs is not necessarily unique, but this is not important in the following.

Lemma 5.1 *The first pair of opposite edges around a degree four Steiner point must be* straight.

Proof. Suppose one of the first pair of opposite edges, say (s, v_1), is a bent edge with a single corner point c_1 (under a suitable embedding). Then s is a degree four Steiner point for c_1, v_2, v_3 and v_4. But s_1 and c_1 cannot both be collinear with v_3 and s — a contradiction. ∎

The second pair of opposite edges has a slightly relaxed, but still quite restricted form:

Lemma 5.2 *The second pair of opposite edges around a degree four Steiner point uses* adjacent *legal orientations only. Furthermore, let S be the intersection of the shortest path parallelogram $R(v_2, v_4)$ with the first pair of opposite edges (hence S is a segment). Then $|v_2 s'|_{\mathcal{D}}$ is the same for any point $s' \in S$; similarly, $|v_4 s'|_{\mathcal{D}}$ is the same for any point $s' \in S$.*

Proof. Consider any embedding of the second pair of opposite edges such that sv_2' is a straight segment of the edge (s, v_2), and sv_4' is a straight segment of the edge (s, v_4). Assume that sv_2' and sv_4' use different legal orientations (if no such

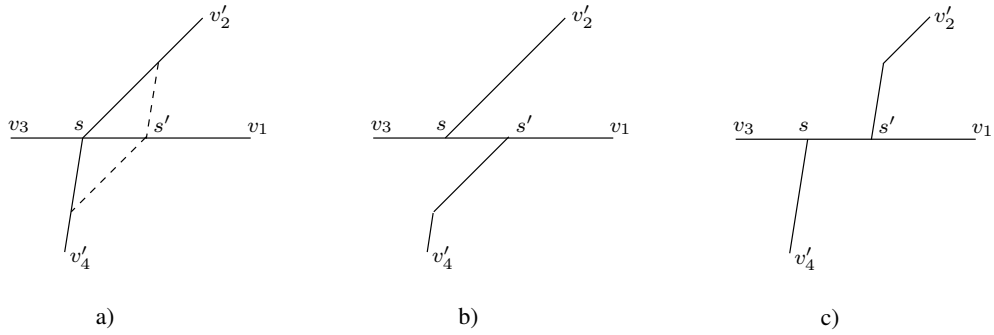

Figure 10: Degree four Steiner point. a) Movement of s to point s' on the first pair of opposite edges. b) Splitting into degree three Steiner points (option one). c) Splitting into degree three Steiner points (option two).

embedding exists, then the lemma trivially holds since then both edges are straight and collinear).

Now we can move s to another point s' on the first pair of opposite edges, such that we connect s' to the segment sv_2' using the legal orientation of segment sv_4', and vice versa (Figure 10a). Clearly, this operation does not change the length of the tree, and it introduces the two legal orientations on the opposite edges. Hence the edges (s, v_2) and (s, v_4) must use adjacent legal orientations, and the path from v_2 to v_4 across s is a shortest path from v_2 to v_4.

For the second part of the lemma, note that as we move Steiner point s to the new point s', we clearly have $|v_2s|_{\mathcal{D}} + |v_4s|_{\mathcal{D}} = |v_2s'|_{\mathcal{D}} + |v_4s'|_{\mathcal{D}}$. Thus, if $|v_2s'|_{\mathcal{D}} > |v_2s|_{\mathcal{D}}$, then $|v_4s'|_{\mathcal{D}} < |v_4s|_{\mathcal{D}}$. Hence we can keep the connection from v_2 to s and use the connection from v_4 to s', thus reducing the length of the tree — a contradiction. ∎

A consequence of this lemma is that if the second pair of opposite edges are not straight *and* collinear, then we can always split the Steiner point s into a pair of adjacent degree three Steiner points. In fact, this split can be made in two topologically different ways as indicated in Figures 10b and 10c.

Define a *cross* as a degree four Steiner point where both the first and second pair of opposite edges are straight and collinear. So far we have shown that unless the degree four Steiner point is a cross, we can always split it into two adjacent degree three Steiner points. We will now show that even if the Steiner point is a cross, then in most cases we can still split it into two degree Steiner points. First we prove an intermediate result that turns out to be helpful in later parts of the paper.

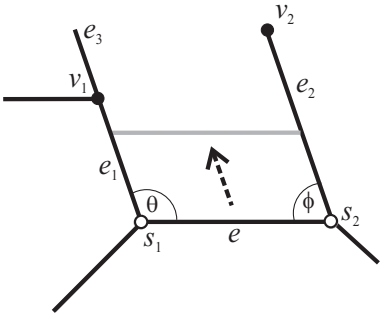

Figure 11: A slide on the edge e.

Lemma 5.3 *Let $e = (s_1, s_2)$ be an edge connecting two Steiner points (s_1 and s_2) in a fulsome SMT T. Let $e_1 = (s_1, v_1)$ be the next edge incident with s_1 travelling counter-clockwise from e, and let $e_2 = (s_2, v_2)$ be the next edge incident with s_2 travelling clockwise from e. Then there exists an embedding of T such that θ, the angle at s_1 between e and e_1, and ϕ, the angle at s_2 between e and e_1, satisfy $\theta + \phi > \pi$.*

Proof. For the given embedding of T, let $\mathbf{u}_1$ be the outward direction of e_1 at s_1 and let $\mathbf{u}_2$ be the outward direction of e_2 at s_2. Observe that

$$\theta + \phi \geq \pi \tag{1}$$

since otherwise we could simultaneously perturb s_1 in direction $\mathbf{u}_1$ and s_2 in direction $\mathbf{u}_2$ decreasing $|s_1 s_2|$ and hence decreasing $|T|_{\mathcal{D}}$, which contradicts minimality.

Now suppose that the lemma does not hold; in other words, that $\theta + \phi = \pi$, as illustrated in Figure 11. Then we can perform a *slide* on e, by which we mean a simultaneous movement of s_1 in direction $\mathbf{u}_1$ and s_2 in direction $\mathbf{u}_2$ (at the same speed), without increasing the length of T. (This is an example of a *zero-shift*, which we study in more detail in Section 6.) Note that neither e_1 nor e_2 contains a corner point, since otherwise there would exist an alternative embedding of the edge, which, by equation (1), would have a larger angle at s_1 or s_2. It follows that we can continue to slide e until either s_1 coincides with v_1 or s_2 coincides with v_2.

Assume, without loss of generality, that s_1 coinciding with v_1 occurs first. If v_1 is a terminal then we have a contradiction to T being fulsome. If v_1 is a Steiner

point then let θ_1 be the meeting angle at v_1 between e_1 and the next edge e_3 going counter-clockwise around v_1 from e_1. By Theorem 3.2, $\theta_1 \leq \pi$. If $\theta_1 < \pi$ then there exists an embedding of e_3 such that continuing to slide e past v_1 strictly decreases the length of e, contradicting the minimality of T. Hence $\theta_1 = \pi$, and e_3 is a straight edge. We can now continue to slide e past v_1 without increasing $|T|_{\mathcal{D}}$. The same argument applies at each Steiner point encountered. Hence we can continue the slide until we reach a terminal, giving a contradiction to T being fulsome. ∎

A consequence of this lemma is that in a fulsome SMT we cannot have a pair of parallel straight edges that are connected by a third edge.

Theorem 5.4 *In a fulsome SMT, a degree four Steiner point can always be split into two adjacent degree three Steiner points* unless *it is a cross and is adjacent to terminals only.*

Proof. By the comment following Lemma 5.2, we only need to consider the case where the Steiner point s is a cross. Assume that one of the neighbours of s is a Steiner point v, and that v has degree three. By Lemma 5.3, there exists an embedding of the SMT such that neither of the line segments va and vb connecting v to the two neighbours other than s are parallel to the straight edges incident to s (Figure 12a). Hence we can make the (small) local change indicated in Figure 12b without increasing the length of the tree. This change will split s into two adjacent degree three Steiner points s_1 and s_2 while moving v to a new position v'.

Now, if v was a degree four Steiner point, then we arrive at a contradiction to length-minimality, since the local change given above would decrease the length of the tree. ∎

In the remainder of this paper we will therefore assume that there always exists an embedding of a full and fulsome SMT where all Steiner points have degree three. (The construction of a cross with terminals as neighbours can easily be handled separately.)

5.2 Direction Sets for Full SMTs

Let T be a full and fulsome SMT where all Steiner points have degree three. We begin by describing a (not necessarily unique) method of colouring the edges of T.

Pick any Steiner point s and any feasible coloured direction set $\mathcal{U}$ for s. The direction set $\mathcal{U}$ defines a colour for each of the edges incident with s, and these appear as red, green and blue in counter-clockwise order around s. Now pick any

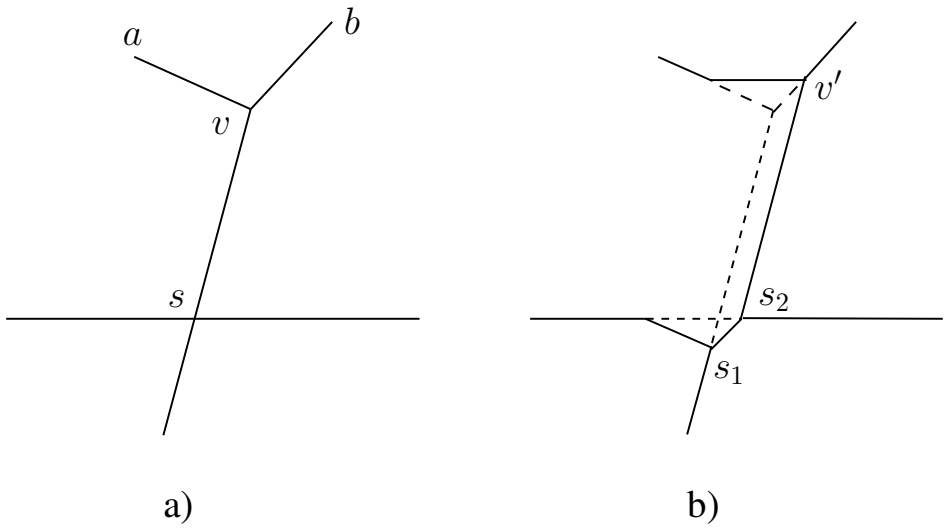

Figure 12: Splitting of a cross into two adjacent degree three Steiner points.

Steiner point neighbour s' of s. Again assume that the colours appear in counter-clockwise order as red, green and blue around s'; thus the single coloured edge incident with s' uniquely defines the colours of the other two edges. Repeat this procedure until all edges of T have been coloured.

We also assign a parity to the vertices of T depending on whether the path in T from s to that vertex contains an odd or even number of edges. Since T is a tree, this assignment of parity is well defined. When we in the following say that there exists a single direction set $\mathcal{U}$ that is used by all Steiner points of T, the interpretation should be that the direction set $\mathcal{U}$ is used at even vertices while the complementary direction set of $\mathcal{U}$ is used at odd vertices.

Theorem 5.5 *Given a full and fulsome SMT, there exists a single direction set that is used by every Steiner point in the tree.*

Proof. We prove the theorem by showing that, given any two adjacent Steiner points s_1 and s_2 in a full and fulsome SMT, there exists a single direction set that is used by s_1 and s_2, and furthermore there exists a small finite perturbation of s_1 and s_2 such that the resulting tree is still a full SMT and the directions used by the edges incident with s_1 exactly coincide with the directions used by the edges incident with s_2. This means that the direction set at any Steiner point can be propagated throughout the SMT, since all internal nodes of the full SMT are Steiner points. The theorem then immediately follows.

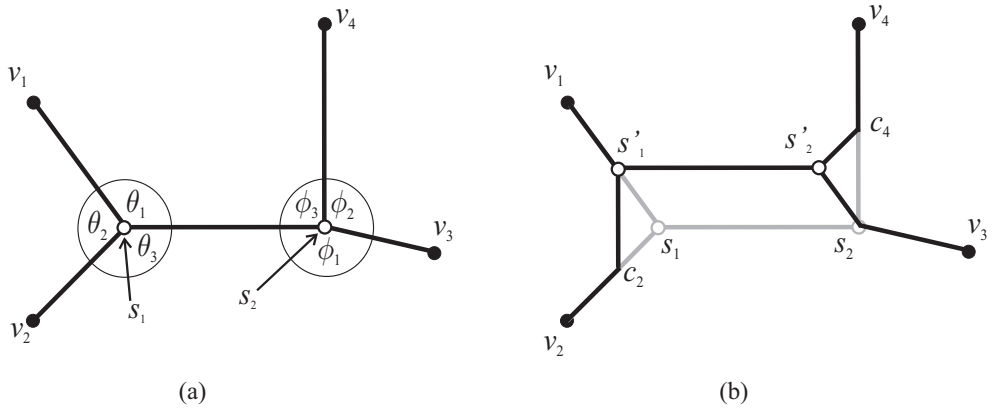

Figure 13: Performing a shift on adjacent Steiner points.

Let s_1 and s_2 be adjacent Steiner points in a full and fulsome SMT. For a given embedding of this SMT, let v_1 and v_2 be the nodes or corner points adjacent to s_1 on the other two incident edges, travelling counter-clockwise from s_1s_2, ie, line segments s_1v_1 and s_1v_2 each use a single legal orientation. Similarly, let v_3 and v_4 be the nodes or corner points adjacent to s_2 on the other two incident edges, travelling counter-clockwise from s_2s_1. Let T be the resulting full SMT on terminal set $\{v_1, v_2, v_3, v_4\}$ with Steiner points s_1 and s_2. This is illustrated in Figure 13a. Let $\mathbf{u}_1$ and $\mathbf{u}_2$ be the directions of $\overrightarrow{s_1v_1}$ and $\overrightarrow{s_1v_2}$ respectively, and let $\mathbf{u}_3$ and $\mathbf{u}_4$ be the directions of $\overrightarrow{s_2v_3}$ and $\overrightarrow{s_2v_4}$ respectively.

For simplicity, we assume either that s_1s_2 is a straight edge or that it is embedded using two corner points (as in Figure 2b), so that both ends of the edge use the same direction. Let $\theta_1, \theta_2, \theta_3$ be the three angles around s_1, travelling counter-clockwise from s_1s_2, and let ϕ_1, ϕ_2, ϕ_3 be the three angles around s_2, travelling counter-clockwise from s_2s_1. Again, this is illustrated in Figure 13a. By Lemma 5.3, we can choose the embedding of the original full SMT such that

$$\theta_1 + \phi_3 > \pi. \tag{2}$$

Suppose that

$$\theta_3 > \phi_3. \tag{3}$$

Under this assumption, we construct a transformation on T that does not increase its length. We do this by defining a *shift* on s_1 and s_2 (shifts will be discussed

in more generality in the next section). This involves moving each of s_1 and s_2 a distance ε in direction $\mathbf{u}_1$ to s_1' and s_2' respectively, where $\varepsilon > 0$ is small compared to all edge lengths in T.

We claim that we can construct a line segment from s_1' in direction $-\mathbf{u}_4$ meeting s_1v_2 at a point c_2. For such a construction to be possible, for sufficiently small ε, we require that the ray from s_1 in direction $\mathbf{u}_2$ must intersect the ray from s_1' in direction $-\mathbf{u}_4$. This occurs if $\phi_3 \geq \pi - \theta_1$ and $\phi_3 < \theta_3$ which follow from inequalities (2) and (3), respectively. Similarly, we can construct a line segment from s_2' in direction $-\mathbf{u}_2$ meeting s_2v_4 at a point c_4. Furthermore, c_4 does not coincide with s_2' since inequality (2) is a strict inequality.

Now, construct a new tree T' interconnecting $\{v_1, v_2, v_3, v_4\}$ via Steiner points s_1' and s_2', such that c_2 is the corner point of the edge $s_1'v_2$, c_4 is the corner point of the edge $s_2'v_4$ and s_2 is the corner point of the edge $s_2'v_3$. The remaining external edge, $s_1'v_1$, is a straight edge. This is illustrated in Figure 13b.

We next observe that $\|T'\| = \|T\|$. To see this, note that in transforming T to T' the edge s_1s_2 and line segments s_1s_1', s_1c_2 and s_2c_4 have been removed, and the edge $s_1's_2'$ and line segments s_2s_2', $s_2'c_4$ and $s_1'c_2$ have been added. But $\|s_1s_2\| = \|s_1's_2'\|$ (since s_1 and s_2 undergo identical translations),$\|s_1s_1'\| = \|s_2s_2'\|$ (by construction) and $\|s_1c_2\| = \|s_2'c_4\|$, $\|s_2c_4\| = \|s_1'c_2\|$ (since triangles $\Delta s_1s_1'c_2$ and $\Delta s_2's_2c_4$ are congruent). Hence, $\|T'\| = \|T\|$. In other words, T' is also a full SMT on the terminal set of T.

We now show that there is a single direction set that is used by s_1 and s_2 in the original full SMT, and that by performing a pair of shifts as described above we can construct a new SMT such that the directions used by the edges incident with s_1 exactly coincide with the directions used by the edges incident with s_2. We do this by showing that, for each of the three colour labels for edges, the direction sets for s_1 and s_2 coincide on that colour and we can ensure that all directions are used at each Steiner point. Note that this is trivially true for the colour of the edge s_1s_2. Now, observe that the edges (or half-edges) s_1v_2 and s_2v_4 are labelled with the same colour (say, blue). If both these line segments use the same direction for every embedding then the direction sets for s_1 and s_2 coincide on the blue colour. If there exists an embedding such that s_1v_2 and s_2v_4 have different directions then either $\theta_3 > \phi_3$ or $\phi_3 > \theta_3$. In either case we can perform the local transformation above (swapping the roles of s_1 and s_2 if necessary) resulting in a new SMT that uses both blue directions at s_1' and s_2'. In order for this new tree to be minimal (under any embedding of the original tree) it again follows that the direction sets for s_1 and s_2 coincide on the blue label, and that both directions are used by both edges after applying the transformation. The same argument applies to the

remaining colour label, concluding the proof. ∎

This theorem is similar in spirit to the result of Du et al. [10] for metrics defined by strictly convex and differentiable unit circles, which says that edges of a full SMT use exactly three different orientations. A corollary of our theorem is that the edges of a full and fulsome SMT for a metric defined by a polygonal unit circle use at most 6 legal orientations. In the following section we show that 4 legal orientations actually suffice.

6 Length-Preserving Shifts and Canonical Forms

The efficiency of the algorithms that we develop in this paper for constructing SMTs comes from the fact that we can assume that full SMTs have particular canonical forms. Our means of establishing these canonical forms is to use the properties of length preserving perturbations, denoted zero-shifts, which we describe in this section.

Given a weighted set of legal orientations defining a normed plane, let the ordered subset $\mathcal{U} = \{\mathbf{u}_1, \mathbf{u}_2, \ldots, \mathbf{u}_k\}$ be a *coloured* direction set, as defined in Section 4. The elements of $\mathcal{U}$, treated as vectors rooted at the origin, appear in counterclockwise order, beginning with $\mathbf{u}_1$, which corresponds to the exclusively primary red direction, and $\mathbf{u}_2$, which corresponds to the exclusively secondary red direction. By Lemma 4.1 we know that $k = 4, 5$ or 6. We define the *direction weight set* of $\mathcal{U}$ to be the set $\{w_1, w_2, \ldots, w_k\}$ where each $w_i = 1/|\mathbf{u}_i|$ (where the norm $|\cdot|$ is the usual Euclidean norm). We define the *direction angle set* of $\mathcal{U}$ to be the set $\{\theta_1, \theta_2, \ldots, \theta_k\}$ where each θ_i is the angle between $\mathbf{u}_i$ and $\mathbf{u}_{i+1}$ (where addition in the subscripts is modulo k). Hence, for each $i \in \{1, \ldots, k\}$ we have $\cos\theta_i = w_i w_{i+1}(\mathbf{u}_i \cdot \mathbf{u}_{i+1})$. Note that the direction angle set must also satisfy the condition that $\sum_{i=1}^{k} \theta_i = 2\pi$.

6.1 Fundamental Zero-shifts and Their Applications

For a given coloured direction set $\mathcal{U}$, let T be a full and fulsome SMT. Furthermore, assume that the edges of T uses all directions in $\mathcal{U}$.

We define a *zero-shift* as a perturbation of one or more Steiner points in T such that the perturbation does not increase the length of T. Such a perturbation $\mathbf{v}$ is called a *fundamental zero-shift* if it cannot be decomposed into two zero-shifts each of which acts on a subset of the Steiner points acted on by $\mathbf{v}$, and at least one of which acts on a proper subset of those Steiner points. Here we will investigate

those fundamental zero-shifts that act on either one Steiner point or two adjacent Steiner points in T. In Section 6.2 we will in fact show that these are the only fundamental zero-shifts that can occur in T.

Let s be a Steiner point in T such that the edges incident with s use all directions in $\mathcal{U}$. Clearly, for any $\mathcal{U}$, there exists a T that contains such a Steiner point; for example, we can construct a suitable SMT T with a single Steiner point.

We now consider properties of 1-point fundamental zero-shifts for s. We will show that such a perturbation can exist only under very special conditions.

Lemma 6.1 *Suppose the direction set $\mathcal{U}$ of T contains exactly 4 directions. Then there are no 1-point zero-shifts for any Steiner points in T.*

Proof. Let s be a Steiner point in T. We first show that the angle θ between the blue and green directions is strictly less than π.

Suppose, on the contrary, that $\theta = \pi$. Consider the SMT T' consisting of the edges in T incident with s and their end points, where the terminals, v_1, v_2, v_3, of T' are the three neighbours of s. Let (v_1, s) be the red edge of T'. Since $\theta = \pi$, it follows that v_2, s and v_3 are collinear. By a continuity argument, similar to the argument in the proof of Lemma 4.1, a sufficiently small perturbation of v_2 off the line through v_2 and v_3 will result in only a small bounded perturbation of s. After applying this perturbation, the green and blue edges will use their existing directions but require at least one extra direction in order to intersect close to s. This means that $\mathcal{U}$ contains at least 5 directions, giving a contradiction.

Hence, $0 < \theta < \pi$. It follows that the position of s is uniquely determined by the positions of the two adjacent vertices incident with the green and blue edges, and thus there can be no 1-point zero-shift of s. ∎

If $\mathcal{U}$ contains 5 directions then the following lemma holds:

Lemma 6.2 *Suppose $\mathcal{U}$, the direction set for T, contains exactly 5 directions, i.e., $\mathcal{U} = \{\mathbf{u}_1, \ldots, \mathbf{u}_5\}$. Let s be a Steiner point in T using all directions in $\mathcal{U}$. Without loss of generality, we assume that there are two red directions and two green directions. Let $\{w_1, w_2, \ldots, w_5\}$ and $\{\theta_1, \theta_2, \ldots, \theta_5\}$ be the direction weight set and direction angle set, respectively, of $\mathcal{U}$. Then:*

(1) there exist 1-point fundamental zero-shifts for s, perturbing s in the directions of $\mathbf{u}_5$ and $-\mathbf{u}_5$;

(2) the following condition holds for $\mathcal{U}$:

$$\frac{w_2 \sin(\theta_5) - w_1 \sin(\theta_1 + \theta_5)}{\sin(\theta_1)} + \frac{w_3 \sin(\theta_4) - w_4 \sin(\theta_3 + \theta_4)}{\sin(\theta_3)} = w_5$$

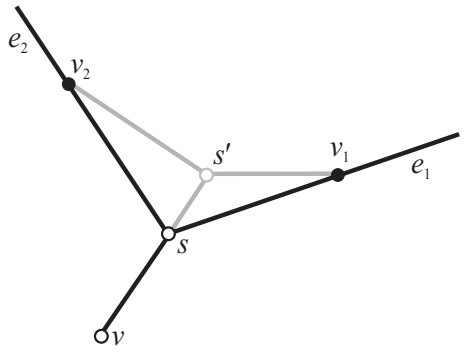

Figure 14: A zero-shift for a Steiner point whose direction set contains five directions.

Proof. Let v be the neighbouring node to s on the blue edge. Since s uses all five directions in $\mathcal{U}$, we can embed the incident red and green edges, each with a single corner point, so that e_1, the red secondary half-edge, is incident with s, and e_2, the green primary half-edge, is also incident with s. This is illustrated in Figure 14.

If we perturb the point s a sufficiently small positive distance in the direction of $-\mathbf{u}_5$ to a point s' we can find points v_1 on e_1 and v_2 on e_2 such that $\overrightarrow{s'v_1}$ is in the red primary direction and $\overrightarrow{s'v_2}$ is in the green secondary direction. Since s and s' both use the direction set $\mathcal{U}$, they are both Steiner points for SMTs with terminals v, v_1, v_2, and the same topology. It follows (from the convexity of the length function under the given norm) that the perturbation from s to s' (and from s' to s) is a zero-shift, proving part (1) of the lemma.

For part (2) we observe that since the two SMTs on v, v_1, v_2 with Steiner points s and s' have the same length, it follows that $|v_1 s|_{\mathcal{D}} + |v_2 s|_{\mathcal{D}} = |v_1 s'|_{\mathcal{D}} + |s s'|_{\mathcal{D}} + |v_2 s'|_{\mathcal{D}}$. Using elementary trigonometry, we can write this in terms of the angles and weights of the direction set to obtain the condition in (2). ∎

Note the the Lemma 6.2 still applies if any of the meeting angles are π. Indeed, in some cases we get slightly stronger results. If $\theta_3 + \theta_4 = \pi$, then it is clear from the degeneracy of the zero-shift that the perturbation can be performed in either direction even if no edge incident with s uses direction $\mathbf{u}_4$. Similarly, if $\theta_1 + \theta_5 = \pi$, then a 1-point fundamental zero-shift can be performed in either direction even if no edge incident with s uses direction $\mathbf{u}_1$.

If $\mathcal{U}$ contains 6 directions then we get the following result:

Lemma 6.3 *Suppose $\mathcal{U} = \{\mathbf{u}_1, \mathbf{u}_2, \ldots, \mathbf{u}_6\}$ is the direction set for T. Let s be a Steiner point in T using all directions in $\mathcal{U}$. Let $\{w_1, w_2, \ldots, w_6\}$ and $\{\theta_1, \theta_2, \ldots, \theta_6\}$ be the direction weight set and direction angle set, respectively, of $\mathcal{U}$. Then:*

(1) for every direction, there exists a 1-point fundamental zero-shift for s, perturbing s in that direction;

(2) the following two conditions hold simultaneously for $\mathcal{U}$:

$$\frac{w_2 \sin(\theta_5 + \theta_6) - w_1 \sin(\theta_1 + \theta_5 + \theta_6)}{\sin(\theta_1)} + \frac{w_3 \sin(\theta_4) - w_4 \sin(\theta_3 + \theta_4)}{\sin(\theta_3)} = w_5$$

and

$$\frac{w_2 \sin(\theta_6) - w_1 \sin(\theta_1 + \theta_6)}{\sin(\theta_1)} + \frac{w_3 \sin(\theta_4 + \theta_5) - w_4 \sin(\theta_3 + \theta_4 + \theta_5)}{\sin(\theta_3)} = w_6.$$

Proof. This is an easy corollary to Lemma 6.2. The two conditions in part (2) are obtained by considering zero-shifts in the primary and secondary blue directions respectively. Since these two directions are linearly independent it follows that every direction is a linear combination of the two blue directions. Hence there exist 1-point fundamental zero-shifts for s in every direction, obtained by taking a suitable combination of zero-shifts in the two blue directions. ∎

Note that, by symmetry, we can obtains equivalent conditions to those in Lemma 6.3(2) by subtracting 2 or by subtracting 4 from every subscript in the equations (where the subtractions are performed modulo 6). These new conditions however do not impose any extra constraints upon the direction set, but rather can be derived from the two conditions given in the lemma.

Next, we consider properties of 2-point fundamental zero-shifts for T. The results here are very similar to those in [6], and hence only require a brief discussion.

Lemma 6.4 *Let s_1 and s_2 be neighbouring Steiner points in T. Assume that (s_1, s_2) is a straight edge which is neither exclusively primary nor exclusively secondary. Let e_1 and e_2 be distinct edges of T incident with s_1 and s_2 respectively, such that e_1 and e_2 have the same colour. Assume that for at least one of $i = 1$ or $i = 2$ the meeting angle between the two edges other than e_i at s_i is not*

π. For each $i \in \{1, 2\}$ let v_i be the closest neighbouring node or corner point on e_i to s_i. If $\overrightarrow{s_1 v_1}$ and $\overrightarrow{v_2 s_2}$ have different directions then there exists a 2-point fundamental zero-shift for s_1 and s_2.

This lemma follows immediately from the proof of Theorem 5.5, using the construction illustrated in Figure 13. Note that the condition on (s_1, s_2) means that the direction set of T contains at most 5 directions. It follows that there are no 1-point zero-shifts that move s_1 or s_2 in the same direction as the constructed 2-point zero-shift, and hence that the 2-point zero-shift is fundamental.

The remaining 2-point zero-shift not covered by Lemma 6.4 is where T necessarily contains meeting angles of π at both s_1 and s_2, in each case between the two incident edges other than e_1 or e_2. This implies that all edges incident with s_1 and s_2 other than e_1 and e_2 are straight and collinear. In this case, the resulting 2-point zero-shift is no longer fundamental, but can be decomposed into two 1-point zero-shifts, by the same argument used in the proof of Lemma 5.2.

We conclude this section by proving two important properties of full and fulsome SMTs that follow from the above properties of fundamental zero-shifts.

Lemma 6.5 *Let s be a Steiner point in a fulsome SMT T. Let u, v and w be the three neighbouring nodes of s in T, and suppose the edges (s, u) and (s, v) are straight and s, u and v are collinear. Then w is a terminal.*

Proof. Let $\mathbf{u}$ and $-\mathbf{u}$ be the directions of the edges (s, u) and (s, v). We prove the lemma by contradiction.

Assume w is not a terminal, and let a and b be the other two neighbouring nodes of w. Suppose one of these nodes (say, a) has the property that the edge between w and that node, (w, a), is straight and has direction $\mathbf{u}$ or $-\mathbf{u}$. Then, by Lemma 5.3, we obtain a contradiction to T being a fulsome SMT.

If, on the other hand, neither (w, a) nor (w, b) is straight with direction $\mathbf{u}$ or $-\mathbf{u}$, then it follows that the direction set for T contains at least 5 directions, with two directions for each of the two colours associated with (s, u) and (s, v). Hence, by Lemmas 6.2 and 6.3, there exists a 1-point zero-shift on w which we can continue to apply until either (w, a) or (w, b) is straight with direction $\mathbf{u}$ or $-\mathbf{u}$. Hence we again obtain the same contradiction as above. ∎

A consequence of Lemma 6.5 is the following theorem which gives strong restrictions on when degree four Steiner points can occur as part of a fulsome SMT.

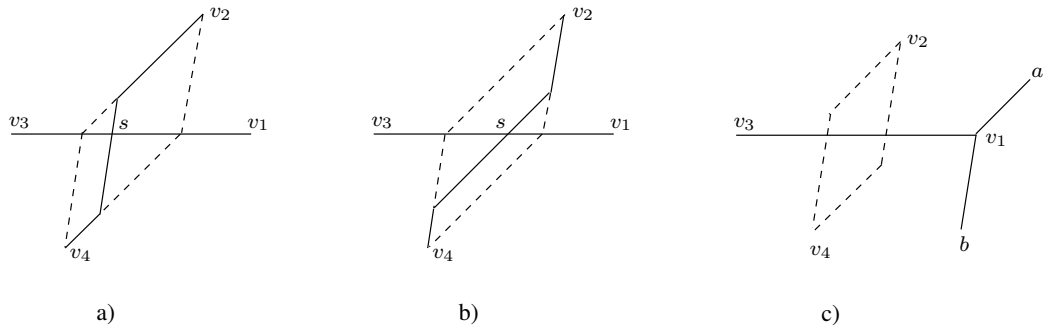

Figure 15: Illustration of observations for proving that a degree four Steiner point in a fulsome SMT must be a cross.

Theorem 6.6 *In a fulsome SMT, a degree four Steiner point must be a cross,* unless *it is adjacent to terminals only.*

Proof. Consider a degree four Steiner point s with neighbours v_1, v_2, v_3 and v_4 which does not form a cross, that is, the second pair of opposite edges, (s, v_2) and (s, v_4), are not straight and collinear (as in Figure 10).

The fact that vertices v_2 and v_4 must be terminals follows by splitting the Steiner point s into two adjacent degree three Steiner points and applying Lemma 6.5.

Before we prove that v_1 and v_3 also must be terminals, we make a few observations. Let S be the line segment between v_1 and v_3. By moving s along S, we can always make the second pair of opposite edges *locally collinear* in two different ways as shown in Figure 15a and Figure 15b. As a consequence, the vertex v_1 cannot be degree four Steiner point, since then we could construct a pair of locally collinear edges around s and v_1, respectively, but the collinear edges of s and v_1 would be non-parallel — hence making a length-decreasing shift of the edge (s, v_1) feasible.

So we may assume that v_1 is a degree three Steiner point. By splitting s into degree three Steiner points in the two topologically different ways shown in Figure 10b and 10c, and applying Theorem 5.5, it follows that the two edges (v_1, a) and (v_1, b) incident to v_1 (other than (v_1, s)) must use the same pair of adjacent legal orientations as (s, v_2) and (s, v_4). Therefore, if one of the edges (v_1, a) or (v_1, b) is a bent edge, then we can always construct a pair of locally collinear edges at v_1. This again leads to a contradiction to length-minimality by using the same arguments as in the degree four case.

As a consequence, we are left with the case where the edges (v_1, a) and (v_1, b) are straight and not collinear (Figure 15c). However, it is always possible to move

s along S to a point s' where either (s', v_2) is straight and parallel to (v_1, a) — or (s', v_4) is straight and parallel to (v_1, b). In both cases, by Lemma 5.3 we arrive at a contradiction to fulsomeness. ∎

6.2 General Zero-shifts

The following lemma gives conditions for the existence of general zero-shifts, and establishes a key property of such shifts: informally, that they can move exclusively primary or exclusively secondary material from one edge to another. This lemma is the key tool for constructing the canonical forms in Section 6.3.

Theorem 6.7 *Let e_1 and e_2 be two edges in a full and fulsome SMT T such that e_1 has an exclusively secondary component and e_2 has an exclusively primary component. Then there exists a zero-shift acting on the Steiner points on the path from e_1 to e_2 in T, such that the shift can continue to be performed until either e_1 has no exclusively secondary component or e_2 has no exclusively primary component. Furthermore, this shift preserves the direction of all straight edges except (possibly) e_1 and e_2.*

Proof. Let s_1 and s_2 be, respectively, the first and last Steiner points on the path from e_1 to e_2 in T. For each $i \in \{1, 2\}$ let θ_i be the meeting angle at s_i between the two incident edges other than e_i.

Case 1. For $i = 1$ or $i = 2$ assume that the two edges incident with s_i are straight edges and $\theta_i = \pi$. In that case there is a 1-point zero-shift moving s_i along the line through those other two edges (as in the proof of Lemma 5.2). Assume first that T spans at least five terminals. If the moving Steiner point s_i meets another Steiner point without the edge e_i becoming straight, then this is a contradiction to fulsomeness by Theorem 6.6. Next assume that T spans four terminals or less. If a Steiner point s_i meets another Steiner point, then in fact we must have $s_1 = s_2$ (the tree T is a star). In this case we can move the overlapping Steiner points s_1 and s_2 jointly as indicated in the proof of Theorem 6.6 (see also Figure 15). Hence it is always possible either to make e_1 exclusively primary or to make e_2 exclusively secondary.

Case 2. If Case 1 does not apply then we argue by induction (as in Theorem 4.1 of [6]). As a first step, we show that the theorem holds for those cases where there are at most two Steiner points in the path from e_1 to e_2, in other words, for 1-point and 2-point zero-shifts. We also show that in each of these cases the

zero-shift strictly decreases the ratio of secondary material to primary material in e_1 and and strictly increases it in e_2.

Case 2.1: 1-point zero-shifts. This case occurs where e_1 and e_2 are both incident with the same Steiner point s, that is, $s_2 = s_1 = s$. This is the same as the situation illustrated in Figure 14. Let v be the neighbouring vertex to s_1 that is not an endpoint of e_1 or e_2. The zero-shift either moves s away from or towards v. If s moves away from v then the lemma clearly holds. If s moves towards v then the only problem that can occur is that the moving Steiner point may meet v before either e_1 or e_2 is straight. But in that case T is either not fulsome (if v is a terminal) or we have two adjacent bent edges incident with a degree four Steiner point, which is a contradiction to T being a SMT, by Lemma 5.1.

Case 2.2: 2-point zero-shifts. This case occurs where e_1 and e_2 are incident with neighbouring Steiner points, s_1 and s_2. Firstly, suppose that e_1 and e_2 both have the same colour. Then the 2-point zero-shift is a fundamental zero-shift, of the sort illustrated in Figure 13b (where $(s_1, v_2) = e_1$ and $(s_2, v_4) = e_2$). This zero-shift acts to decrease the the length of one of the edges e_0 incident with s_1 and s_2 but not on the path from e_1 to e_2 (where $(s_1, v_1) = e_0$ in the figure). It immediately follows that the lemma holds, unless the length of e_0 decreases to 0 before either e_1 or e_2 is straight. However, in such a case the tree contains a degree four Steiner point with an incident bent edge, and a second Steiner point, giving a contradiction to minimality by Theorem 6.6.

Suppose, on the other hand, that e_1 and e_2 have different colours. Let e_0 be the edge incident with s_1 with the same colour as e_2. If e_0 is exclusively primary, then an appropriate zero-shift can be constructed as follows. We can apply a small 1-point zero-shift at s_1, effectively transferring an arbitrarily small exclusively secondary component to e_0. More specifically, it strictly reduces the secondary/primary material ratio in e_1, and increases it in e_0. Now there exists a fundamental 2-point zero-shift between the secondary component of e_0 and the edge e_2. Because the secondary component of e can be assumed to be arbitrarily small, it follows that this second shift can reduce the secondary component of e_0 to 0. Hence, together these two shifts give a zero-shift on the path between e_1 and e_2, that preserves the direction of e_0. The only remaining subcase is where e_0 has an exclusively secondary component, in which case we apply a similar argument, but reverse the order of the two fundamental zero-shifts.

We now conclude the argument by induction on the number of Steiner points in the path between e_1 and e_2, using the method of proof of Theorem 4.1 of [6], which essentially generalises the construction in the previous paragraph. An im-

portant thing to note, in the inductive step, is that we can always find an edge e_0 with exclusively primary or exclusively secondary material and incident with some s_0 on the path between s_1 and s_2 such that the condition of Case 1 ($\theta_0 = \pi$) does not apply at s_0. This means that the required increase and decrease in secondary/primary material ratio occurs in the smaller zero-shift by the inductive assumptions. The induction argument now follows easily. ∎

Note that an immediate corollary of the proof of Theorem 6.7 is that any zero-shift, other than the fundamental zero-shifts described in Section 6.1, can be decomposed into two zero-shifts at least one of which acts on a strictly smaller set of Steiner points. Hence, the only fundamental zero-shifts are those described in Section 6.1.

6.3 Canonical Forms

The existence of zero-shifts makes it possible to transform any full and fulsome SMT into another SMT with the same topology that has some well-defined canonical form. In this section we outline the canonical forms proposed in [5] for the uniform orientation metric and show that they also apply to Steiner trees for the fixed orientation metric.

Definition 6.1 *Given an ordering of the edges in a full Steiner topology $\mathcal{T}$, an SMT T for topology $\mathcal{T}$ is said to be* canonical *with respect to that ordering if T contains at most one bent edge and all primary edges and half-edges of T come before secondary edges and half-edges of T under the ordering.*

In a canonical tree there therefore exists a so-called *transition edge* (which is possibly a bent edge), such that all edges that appear before the transition edge wrt. the given ordering are *primary* and all edges appear after the transition edge are *secondary*. Hence a canonical tree has at most one bent edge.

The proof of the following theorem follows immediately from the fact that we can use zero-shifts to move primary/secondary components between edges in T. (A detailed proof is given in [5], and it works without modifications for the more general fixed orientation case.)

Theorem 6.8 *Let a set terminals N and a full Steiner topology $\mathcal{T}$ for that set of terminals be given. Suppose there exists a full and fulsome SMT for N with topology $\mathcal{T}$. Then for any ordering of the edges of $\mathcal{T}$ there exists a SMT for N (with topology $\mathcal{T}$) which is canonical with respect to that ordering.*

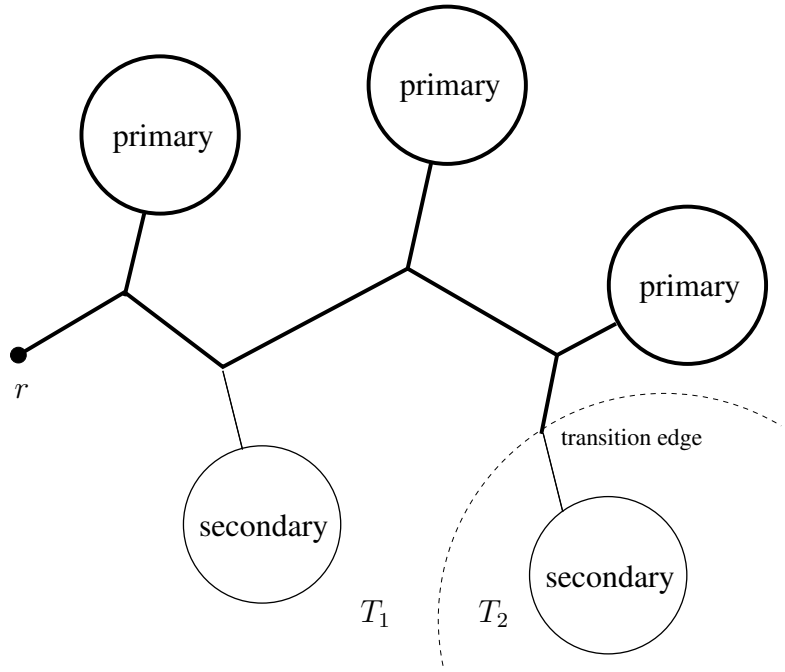

Figure 16: Illustration of a tree T with the depth-first order canonical form. Primary edges are drawn as bold edges, and the remaining edges are secondary edges.

Depending on the chosen ordering, various canonical forms can be obtained [5]. From an algorithmic point of view, the *depth-first ordering* is the most important one: Root $\mathcal{T}$ at some terminal r and order the edges as they appear in a depth-first traversal of the tree from r. This results in a canonical form that is illustrated in Figure 16. If we divide such a canonical tree T into two subtrees T_1 and T_2 by deleting the transition edge, the tree T_2 that does not contain the root is secondary (i.e., all edges in T_2 are secondary edges). Furthermore, the path p from r to the transition edge is primary, while the subtrees that are attached to p either are primary or secondary subtrees. These properties are used by the linear-time algorithm for constructing a SMT for a given topology in Section 7.

By choosing another ordering of the edges, we obtain the following interesting theorem [5]:

Theorem 6.9 *Let T be a full and fulsome SMT for terminal set N with topology $\mathcal{T}$. Then there exists a SMT T' for terminal set N with topology $\mathcal{T}$ that uses at most* four *legal orientations.*

Proof. Order the edges of T by their *colour*; for example, the red edges may come first in the ordering followed by the green edges and then the blue edges. Consider a canonical SMT T' that comes from this ordering (by Theorem 6.8 such a tree exists). Then it follows from the canonical form that the edges of any given colour, not the same as the colour of the transition edge, are either all primary or all secondary. Hence T' uses at most four legal orientations. ∎

Finally, we note that the well-known Hwang canonical form for *rectilinear* trees [12, 23] is a *special case* of the depth-first ordering canonical form. The first observation is that by Lemma 6.5, in a fulsome and canonical rectilinear SMT the topology of a full component must be a *chain* in which every Steiner point is connected directly to at least one terminal. The Hwang topology form is now obtained by rooting the topology in one end of the chain, and constructing the depth-first ordering canonical form. The fact that there can be at most two terminals in the subtree below the bent edge follows from the fullness of the tree.

7 Linear Time Algorithm for a Given Topology

By exploiting the concept of canonical forms, in this section we present a $O(\sigma n)$ time algorithm to compute a full and fulsome SMT T for a given full Steiner topology $\mathcal{T}$ with n terminals (or show that no such tree exists). Our algorithm is a generalisation of the algorithm by Brazil et al. [5] which works for uniform orientation metrics with $\lambda > 3$ given orientations. In the following we denote this the *DFS-canonical algorithm*, since it is based on the canonical form that comes from a depth-first traversal of the topology $\mathcal{T}$. Here we first present the main algorithmic idea in Section 7.1. Then we show that the so-called merging operation can be performed in constant time (Section 7.2), and in Section 7.3 we briefly present the DFS-canonical algorithm and argue that it also works for the general fixed orientation metric.

7.1 Labelling and Merging Algorithm

Consider the topology $\mathcal{T}$ shown in Figure 17. This topology has five terminals $t_1, \ldots, t_5$. We know from Section 5 that there exists a direction set $\mathcal{U}$ that is used by every Steiner point in a full SMT T with topology $\mathcal{T}$ (assuming that such a tree T exists). Assume furthermore that the primary/secondary labelling of the edges in T is as in Figure 17. Hence the edge connecting, e.g., Steiner point s_1 to terminal t_1 is a straight edge with a primary direction from $\mathcal{U}$; however, the

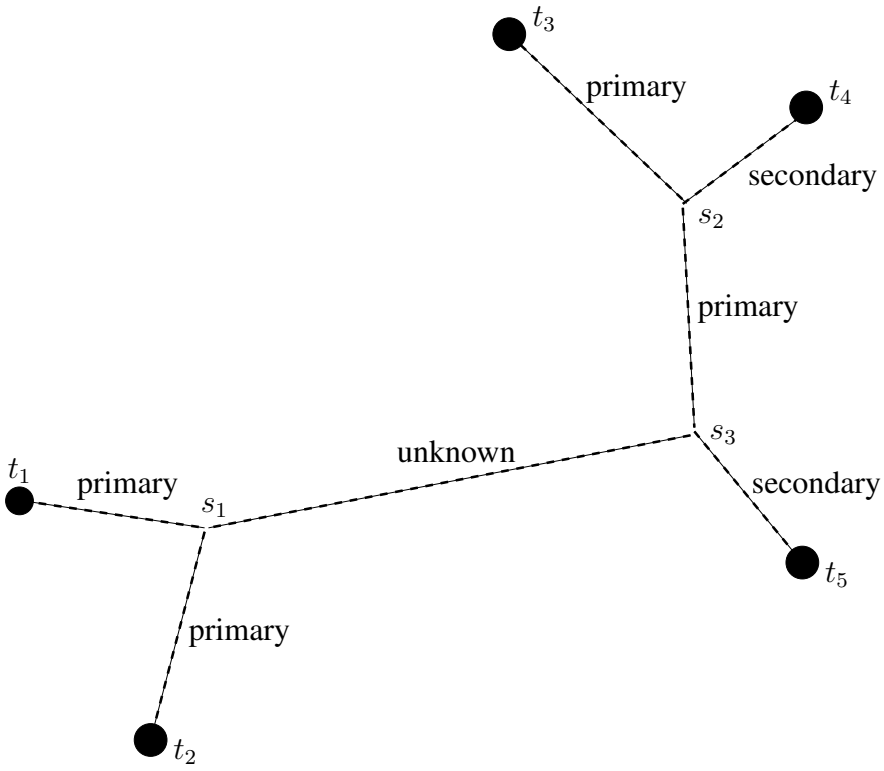

Figure 17: Labelling and bottom-up construction of SMT for a given topology spanning five terminals.

colour of edge (s_1, t_1) is not known. Steiner point s_1 is connected by straight and labelled edges to two nodes (here terminals) with *known* positions. As will be shown in Section 7.2, then in *constant time* we can either compute the *unique* location of s_1 — or decide that s_1 cannot exist with the given direction set and primary/secondary labelling.

The operation of computing the location of a node in $\mathcal{T}$ given the locations of two of its neighbours is called a *merging* operation. If a direction set is given and all edges except one have been labelled primary or secondary (as in Figure 17), then we can compute a tree under this labelling or decide that no such tree exists in $O(n)$ time, where n is the number of terminals in $\mathcal{T}$. We simply root $\mathcal{T}$ at the unlabelled (transition) edge and merge nodes bottom-up in $\mathcal{T}$. In Figure 17 we could, e.g., first compute s_1 based on t_1 and t_2, then s_2 based on t_3 and t_4, then s_3 based on s_2 and t_5, and finally construct the possibly bent transition edge based

on the positions of the Steiner points s_1 and s_3.

This is the main algorithmic idea employed in the linear-time algorithm. By using the canonical forms that come from ordering the edges in $\mathcal{T}$, the number of possible labellings can be reduced from an exponential number — essentially two possible labels per edge in the tree — to a linear number of possible labellings (Section 7.3).

7.2 Constant-time Merging Operation

In this section we present the constant-time merging operation that facilitates the efficient bottom-up construction outlined in Section 7.1. The lemma below was originally proved only for uniform orientation metrics with $\lambda > 3$ [5]; here the lemma is generalised to arbitrary fixed orientation metrics.

Lemma 7.1 *Let T be a full SMT with full Steiner topology $\mathcal{T}$, and let s be a Steiner point in $\mathcal{T}$. Assume that the locations in T of two of the neighbours of s, u and v, are known; furthermore, assume that each edge (s, u) and (s, v) is straight and has been labelled primary or secondary. Finally, assume that we know the direction set for T. If Steiner point s exists in T and is not collinear with u and v, then its location is unique and can be computed in constant time; also, the colours of the edges (s, u) and (s, v) — and hence also the colour of the third edge incident with s — are unique.*

Proof. For the given direction set, we first make the following simple observations:

1. An exclusively primary edge and an exclusively secondary edge of the same colour use adjacent orientations;

2. Every meeting angle is at most π.

Now suppose, contrary to the statement of the lemma, that it is possible to construct two distinct Steiner points s and s' adjacent to both u and v. Direct each incident edge so that it is pointing outwards from s or s'. These incident edges use four (not necessarily distinct) directions, all of which belong to a single direction set. We will consider two cases, each of which show that we reach a contradiction to one of the observations above.

Case 1. Suppose that s and s' are not collinear with u or with v.

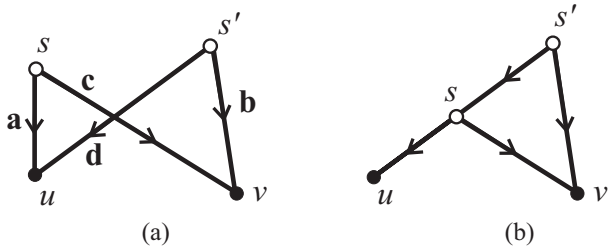

Figure 18: Cases 1 and 2 in the proof of Lemma 7.1.

We will first show that the interiors of two of the edges intersect at a single point. Consider the colours of the four edges (s, u), (s, v), (s', u) and (s', v). Since there are only three colours, at least one colour (say, red) appears twice. Without loss of generality, we can assume that (s, u) is a red edge. Then (s', v) must also be a red edge (since the other edge incident with u has the same primary/secondary labelling as (s, u) but is not collinear, and the two edges incident with s have distinct colours).

We introduce the following vectors (see Figure 18a):

$$\mathbf{a} = \overrightarrow{su},\ \mathbf{b} = \overrightarrow{s'v},\ \mathbf{c} = \overrightarrow{sv},\ \mathbf{d} = \overrightarrow{s'u}.$$

Assume the two red edges (s, u) and (s', v) do not intersect. We will show that the other two edges (s, v) and (s', u) do intersect. Note that this occurs if and only if there exist real numbers $0 < k_1 < 1$ and $0 < k_2 < 1$ satisfying the following condition:

$$\mathbf{a} = k_1\mathbf{c} + k_2\mathbf{d}. \tag{4}$$

Also note that $\mathbf{a} - \mathbf{d} = \mathbf{c} - \mathbf{b}$, that is:

$$\mathbf{a} + \mathbf{b} = \mathbf{c} + \mathbf{d}. \tag{5}$$

First suppose (s, u) and (s', v) both use the same red direction, that is, $\mathbf{b} = k\mathbf{a}$ for some $k > 0$. From equation (5) we obtain: $\mathbf{a} = (\mathbf{c}+\mathbf{d})/(1+k)$ which satisfies condition (4) where $k_1 = k_2 = 1/(k + 1)$.

On the other hand, suppose that (s, u) and (s', v) use different red directions (one exclusively primary and the other exclusively secondary). By Observation 1, these are adjacent orientations, hence $\mathbf{a}$ and $\mathbf{b}$ are linearly independent. This

means there exist $\alpha_1, \alpha_2, \beta_1, \beta_2 \in \mathbf{R}$ such that $\mathbf{c} = \alpha_1\mathbf{a} + \alpha_2\mathbf{b}$ and $\mathbf{d} = \beta_1\mathbf{a} + \beta_2\mathbf{b}$. Since $\mathbf{c}$ and $\mathbf{d}$ do not use red directions, at least one of the α_i's and at least one of the β_i's must be negative. By the symmetry of the equations we can assume, without loss of generality, that $\alpha_2 < 0$. Substituting the expressions for $\mathbf{c}$ and $\mathbf{d}$ into equation (5), we obtain:

$$\mathbf{a} + \mathbf{b} = (\alpha_1 + \beta_1)\mathbf{a} + (\alpha_2 + \beta_2)\mathbf{b},$$

hence $\alpha_1 + \beta_1 = 1$ and $\alpha_2 + \beta_2 = 1$. Since α_2 and at least one of the β_i's are negative, it follows that there exist real numbers $p, q > 0$ such that:

$$\alpha_1 = 1 + p, \;\; \alpha_2 = -q, \;\; \beta_1 = -p, \;\; \beta_2 = 1 + q. \tag{6}$$

Now, suppose we write $\mathbf{a} = k_1\mathbf{c} + k_2\mathbf{d}$. To satisfy condition (4) we need to show that this always has a real solution with $0 < k_1 < 1$ and $0 < k_2 < 1$. Substituting in the expressions for $\mathbf{c}$ and $\mathbf{d}$ we obtain:

$$\mathbf{a} = (k_1\alpha_1 + k_2\beta_1)\mathbf{a} + (k_1\alpha_2 + k_2\beta_2)\mathbf{b}.$$

Using the identities (6) and equating coefficients, we then get the following pair of simultaneous equations:

$$\begin{aligned} k_1(1 + p) + k_2(-p) &= 1 \\ k_1(-q) + k_2(1 + q) &= 0 \end{aligned}$$

Solving for k_1 and k_2 gives

$$k_1 = \frac{1 + q}{1 + p + q}, \;\; k_2 = \frac{q}{1 + p + q},$$

and hence we have $0 < k_1 < 1$ and $0 < k_2 < 1$.

We have now established that the interiors of two of the edges intersect at a single point. We can assume that this pair of intersecting edges is (s, v) and (s', u) (noting that we are no longer carrying across any of the previous assumptions about colours of edges). This is the situation shown in Figure 18a.

If (s, v) and (s', u) are the same colour, then the orientation corresponding to the direction of (s, u) lies strictly between the directions of (s, v) and (s', u) contradicting Observation 1. On the other hand, if (s, v) and (s', u) have different colours, then the remaining two edges must both use the third colour (since the primary and secondary labelling of each edge is known). Hence, the four edges

(s, u), (s, v), (s', u) and (s', v) use three distinct colours. However, the four vertices of the polygonal unit circle $\partial\mathcal{D}$ (centred at the origin) corresponding to the directions of these four edges all lie in one of the open half planes on one side of the line through the origin with direction $\overrightarrow{ss'}$. This means that one of the meeting angles is greater than π, contradicting Observation 2.

Case 2. The remaining possibility is that s and s' are both collinear with exactly one of the points u and v, say u (as in Figure 18b).

Since (s, v) and (s', v) are either both primary or both secondary, it follows that the two edges have different colours, while the edge (s', u) must have the third colour. As in Case 2, these three directions all lie in an open half plane, again contradicting Observation 2.

We conclude that at most one Steiner point can be constructed.

Note that this construction can be done in constant time since the direction set is known. ∎

If s, u and v are collinear, then again the the colours of the edges (s, u), (s, v) and the third edge incident with s are uniquely determined, but the position of s is not unique. This does not cause a problem in the bottom-up construction algorithm due to Lemma 6.5. As a consequence of this lemma, at most one merging operation in the bottom-up construction algorithm can result in a non-unique Steiner point s. In fact, this must then be the final merging operation where the third edge incident to s (in addition to (s, u) and (s, v)) is the *transition* edge, and the other end of this edge is a terminal t. This holds since the construction is moving in towards the transition edge. What we can do here is leave the position of the Steiner point undetermined and construct the transition edge by finding the shortest edge connecting t to the line segment uv. Clearly, this can also be done in constant time like an ordinary merging operation.

7.3 Linear-time DFS-canonical Algorithm

In this section we show how the linear-time construction algorithm from [5] can be generalised to the fixed orientation metric. The algorithm uses the algorithmic idea outlined in Section 7.1, and the constant-time merging operation from Section 7.2. The algorithm is based on the depth-first traversal canonical form, and therefore denoted the DFS-canonical algorithm.

The DFS-canonical algorithm runs in $O(n)$ time for a given direction set $\mathcal{U}$. In Section 4 we showed that the number of possible direction sets is $\Theta(\sigma)$, and

that the direction sets furthermore can be determined in $\Theta(\sigma)$ time. By iterating the $O(n)$ time algorithm over all direction sets, we obtain a total running time of $O(\sigma + \sigma n)$ which is $O(\sigma n)$.

The idea of the DFS-canonical algorithm (for a given topology $\mathcal{T}$ and fixed direction set $\mathcal{U}$) is that if there exists a full and fulsome SMT T with full Steiner topology $\mathcal{T}$ and direction set $\mathcal{U}$, then T can be assumed to have the canonical form that is illustrated in Figure 16. The algorithm consists of two depth-first traversals of $\mathcal{T}$ from an arbitrary root terminal r:

1. Secondary subtrees are constructed bottom-up in $\mathcal{T}$, that is, subtrees where all edges are labelled as secondary edges. The merging operation is performed bottom-up for each Steiner node; if a Steiner point cannot be constructed, then none of the ancestors of the node (relative to r) can constructed either.

2. Primary subtrees are constructed bottom-up in $\mathcal{T}$. At the same time, each edge in $\mathcal{T}$ is tried as potential transition edge. The idea is that it is possible iteratively to construct the endpoints of the transition in constant time per edge: The endpoint that is closest to the root r is constructed in the second traversal, while the other endpoint is constructed in the first traversal of $\mathcal{T}$ (see Figure 16).

Full implementation details are given by Brazil et al. [5]. Thus we have the following theorem:

Theorem 7.2 *Given a full Steiner topology $\mathcal{T}$ with n terminals and a fixed orientation metric with σ legal orientations, then in $O(\sigma n)$ time we can either construct a full and fulsome SMT T with topology $\mathcal{T}$, or decide that no such tree exists.*

8 Conclusion

The main contribution of this paper is to show the existence of powerful canonical forms for SMTs for arbitrary (weighted) fixed orientation metrics. We also gave efficient and simple algorithms to compute all direction sets for a given fixed orientation metric, and to compute a SMT for a given full Steiner topology. Our results show that the two-phase exact algorithm for uniform orientation metrics [15] easily can be adapted to general fixed orientation metrics. This would most likely allow the efficient computation of large-scale SMTs for arbitrary fixed orientation metrics.

Future research would focus on generalising our results further to metrics given by piecewise differentiable unit circles — including proving the conjecture that there in any normed plane and for any set of terminals exists a SMT where the edges of each full component use at most *three* orientations (where the orientation of an edge is defined by the straight line between the endpoints of the edge).

Acknowledgements

This work was partially supported by a grant from the Australia Research Council and by a grant from the Danish Natural Science Research Council (51-00-0336).

References

[1] M. Brazil. Steiner Minimum Trees in Uniform Orientation Metrics. In D.-Z. Du and X. Cheng, editor, *Steiner Trees in Industries*, pages 1–27. Kluwer Academic Publishers, 2001.

[2] M. Brazil, D. A. Thomas, and J. F. Weng. Minimum Networks in Uniform Orientation Metrics. *SIAM Journal on Computing*, 30:1579–1593, 2000.

[3] M. Brazil, D. A. Thomas, and J. F. Weng. Forbidden Subpaths for Steiner Minimum Networks in Uniform Orientation Metrics. *Networks*, 39:186–202, 2002.

[4] M. Brazil, D. A. Thomas, and J. F. Weng. Locally Minimal Uniformly Oriented Shortest Networks. *Discrete Applied Mathematics*, 154:2545–2564, 2006.

[5] M. Brazil, D. A. Thomas, J. F. Weng, and M. Zachariasen. Canonical Forms and Algorithms for Steiner Trees in Uniform Orientation Metrics. *Algorithmica*, 44:281–300, 2006.

[6] M. Brazil, P. Winter, and M. Zachariasen. Flexibility of Steiner Trees in Uniform Orientation Metrics. *Networks*, 46:142–153, 2005.

[7] G. D. Chakerian and M. A. Ghandehari. The Fermat Problem in Minkowski Spaces. *Geometriae Dedicata*, 17:227–238, 1985.

[8] H. Chen, C. K. Cheng, A. B. Kahng, I. I. Mandoiu, Q. Wang, and B. Yao. The Y-Architecture for On-chip Interconnect: Analysis and Methodology. In

Proceedings ACM/IEEE International Conference on Computer-Aided Design (ICCAD), pages 13–19, 2003.

[9] H. Chen, B. Yao, F. Zhou, and C. K. Cheng. The Y-Architecture: Yet Another On-chip Interconnect Solution. In *Proceedings Asia and South Pacific Design Automation Conference*, pages 840–846, 2003.

[10] D.-Z. Du, B. Gao, R. L. Graham, Z.-C. Liu, and P.-J. Wan. Minimum Steiner Trees in Normed Planes. *Discrete and Computational Geometry*, 9:351–370, 1993.

[11] M. Hanan. On Steiner's Problem with Rectilinear Distance. *SIAM Journal on Applied Mathematics*, 14(2):255–265, 1966.

[12] F. K. Hwang. On Steiner Minimal Trees with Rectilinear Distance. *SIAM Journal on Applied Mathematics*, 30:104–114, 1976.

[13] F. K. Hwang, D. S. Richards, and P. Winter. *The Steiner Tree Problem*. Annals of Discrete Mathematics 53. Elsevier Science Publishers, Netherlands, 1992.

[14] H. Martini, K. J. Swanepoel, and G. Weiss. The Fermat-Torricelli Problem in Normed Planes and Spaces. *Journal of Optimization Theory and Applications*, 115:283–314, 2002.

[15] B. K. Nielsen, P. Winter, and M. Zachariasen. An Exact Algorithm for the Uniformly-Oriented Steiner Tree Problem. In *Proceedings of the 10th European Symposium on Algorithms, Lecture Notes in Computer Science*, volume 2461, pages 760–772. Springer, 2002.

[16] M. Sarrafzadeh and C. K. Wong. Hierarchical Steiner Tree Construction in Uniform Orientations. *IEEE Transactions on Computer-Aided Design*, 11:1095–1103, 1992.

[17] K. J. Swanepoel. The Local Steiner Problem in Normed Planes. *Networks*, 36(2):104–113, 2000.

[18] S. Teig. The X Architecture: Not Your Father's Diagonal Wiring. *International Workshop on System-Level Interconnect Prediction (SLIP)*, pages 33–37, 2002.

[19] P. Widmayer, Y. F. Wu, and C. K. Wong. On Some Distance Problems in Fixed Orientations. *SIAM Journal on Computing*, 16(4):728–746, 1987.

[20] X Initiative Home Page. `http://www.xinitiative.com`, 2001.

[21] G. Xue and K. Thulasiraman. Computing the Shortest Network under a Fixed Topology. *IEEE Transactions on Computers*, 51:1117–1120, 2002.

[22] M. C. Yildiz and P. H. Madden. Preferred Direction Steiner Trees. In *Proceedings of the 11th Great Lakes Symposium on VLSI (GLSVLSI)*, pages 56–61, 2001.

[23] M. Zachariasen. Rectilinear Full Steiner Tree Generation. *Networks*, 33:125–143, 1999.

[24] M. Zachariasen. The Rectilinear Steiner Tree Problem: A Tutorial. In D.-Z. Du and X. Cheng, editors, *Steiner Trees in Industries*, pages 467–507. Kluwer Academic Publishers, Boston, 2001.

[25] M. Zachariasen. Comment on "Computing the Shortest Network under a Fixed Topology". *IEEE Transactions on Computers*, 55:783–784, 2006.